

Lehigh University Lehigh Preserve

Theses and Dissertations

1994

Comparison of monochromatic versus directional spectral wave refraction and shoaling analysis for coastal design

Jennifer L. Irish
Lehigh University

Follow this and additional works at: <http://preserve.lehigh.edu/etd>

Recommended Citation

Irish, Jennifer L., "Comparison of monochromatic versus directional spectral wave refraction and shoaling analysis for coastal design" (1994). *Theses and Dissertations*. Paper 251.

This Thesis is brought to you for free and open access by Lehigh Preserve. It has been accepted for inclusion in Theses and Dissertations by an authorized administrator of Lehigh Preserve. For more information, please contact preserve@lehigh.edu.

AUTHOR:

Irish, Jennifer L.

TITLE:

**Comparison of
Monochromatic Versus
Directional Spectral Wave
Refraction and Shoaling
Analysis for Coastal
Design**

DATE: May 29, 1994

**COMPARISON OF MONOCHROMATIC VERSUS
DIRECTIONAL SPECTRAL WAVE
REFRACTION AND SHOALING ANALYSIS FOR
COASTAL DESIGN**

by

Jennifer L. Irish

A Thesis

Presented to the Graduate and Research Committee

of Lehigh University

in Candidacy for the Degree of

Master of Science

in

Civil Engineering

Lehigh University

May 18, 1994

This thesis is accepted and approved in partial fulfillment of the requirements
for the degree Master of Science.

May 17, 1994
Date

~~Thesis Advisor~~

~~Chairperson of Department~~

Acknowledgements

The author is deeply grateful for the guidance and encouragement provided by her advisor, Dr. Robert Sorensen, during the preparation of this thesis as well as throughout her graduate program. Special thanks to Dr. Charles Long of the U.S. Army Corps of Engineers Coastal Engineering Research Center not only for providing the computer models used in this investigation, but also for his invaluable advice and support. Thanks to Mr. Mark Levine for his unparalleled computer expertise and his patience with STWAVE. Thanks also to Ms. Mary Tibbetts for proofreading this report and for lending moral support.

Table of Contents

	Page
List of Figures	vi
List of Tables	viii
Nomenclature	ix
ABSTRACT	1
1.0 INTRODUCTION	3
1.1 Engineering Problem	3
1.2 Scope of Investigation	5
1.3 General Wave Theory Concepts	7
2.0 NUMERICAL APPROACH	11
2.1 RCPWAVE	11
2.1.1 Model Theory	11
2.1.2 Model Assumptions	13
2.1.3 Input Requirements	13
2.1.4 Model Computation	15
2.1.5 Generated Output	17
2.2 STWAVE	17
2.2.1 Model Theory	18
2.2.2 Model Assumptions	20
2.2.3 Model Computation	21
2.2.4 Model Operation	23
2.3 Component Analysis	23
2.3.1 Theory	24
2.3.2 Computation	25
2.3.3 STWAVE Comparison	28
3.0 MODEL EXPERIMENT	30
3.1 Hydrography	30
3.2 Wave Conditions	32
4.0 MONOCHROMATIC WAVE ANALYSIS	34
4.1 Wave Conditions Analyzed	34
4.2 RCPWAVE Analysis	34
4.3 Results	34

	Page	
5.0	DIRECTIONAL SPECTRAL ANALYSIS	36
5.1	Wave Conditions Analyzed	36
5.2	Directional Spectrum Generation	36
5.2.1	Frequency Spectrum	36
5.2.2	Directional Spread	39
5.3	Component Analysis	44
5.3.1	Cosine Squared Directional Distribution	44
5.3.2	Mitsuyasu (1975) Directional Distribution	48
5.4	Results	49
6.0	COMPARISON OF RESULTS	52
6.1	Nearshore Combined Refraction and Shoaling Coefficient	52
6.2	Nearshore Peak Period	56
6.3	Nearshore Mean Propagation Direction	59
7.0	CONCLUSIONS	63
7.1	Impact on Coastal Design	63
7.1.1	Wave Height	63
7.1.2	Wave Period	64
7.1.3	Wave Propagation Direction	64
7.2	Recommendations for Future Analysis	65
	REFERENCES	66
	APPENDIX: Vita	68

List of Figures

	Page
1.1 Basic Design Problem Definition (Sorensen (1993))	4
1.2 Directional Spectrum, Courtesy of the U.S. Army Corps of Engineers Field Research Facility, Duck, North Carolina	6
2.1 Definition of Wave Propagation Direction, θ (Cialone et al. (1992))	14
2.2 RCPWAVE Computational Grid (Cialone et al. (1992))	16
2.3 Definition of Deviance From Mean Propagation Direction, θ	19
2.4 Frequency and Direction Bands for Directional Spectral Analysis	22
2.5 Definition of Representative Frequency and Direction, f_{ij} and θ_{ij}	27
3.1 Beach Profile Factor, A , Versus Sediment Diameter, D , and Fall Velocity, w , (Dean (1987); modified from Moore (1982))	31
3.2 Hypothetical Experiment Site Bathymetry	33
5.1 JONSWAP One-dimensional Spectra Model Distribution	38
5.2 JONSWAP Frequency Spectrum: Deep Water Wave Period - 7 seconds	40
5.3 JONSWAP Frequency Spectrum: Deep Water Wave Period - 12 seconds	41
5.4 Cosine Squared Distribution (Sorensen (1993))	43
5.5 Mitsuyasu (1975) Distribution	45
5.6 Frequency Band Division for the JONSWAP Spectrum with a Cosine Squared Distribution	47

	Page
6.1 Combined Refraction and Shoaling Coefficient Versus Deep Water Mean Propagation Direction: Deep Water Wave Period - 7 seconds	53
6.2 Combined Refraction and Shoaling Coefficient Versus Deep Water Mean Propagation Direction: Deep Water Wave Period - 12 seconds	54
6.3 Nearshore Peak Wave Period Versus Deep Water Mean Propagation Direction: Deep Water Wave Period - 7 seconds	57
6.4 Nearshore Peak Wave Period Versus Deep Water Mean Propagation Direction: Deep Water Wave Period - 12 seconds	58
6.5 Nearshore Mean Propagation Direction Versus Deep Water Mean Propagation Direction: Deep Water Wave Period - 7 seconds	60
6.6 Nearshore Mean Propagation Direction Versus Deep Water Mean Propagation Direction: Deep Water Wave Period - 12 seconds	61

List of Tables

		Page
1	Deep Water Wave Conditions	32
2	Combined Refraction and Shoaling Coefficient - $K_r K_s$ Monochromatic Propagation Analysis	35
3	Nearshore Propagation Direction (deg) Monochromatic Propagation Analysis	35
4	Effective Combined Refraction and Shoaling Coefficient ($K_r K_s$) _{eff} Directional Spectral Propagation Analysis	49
5	Nearshore Mean Spectral Propagation Direction (deg) Directional Spectral Propagation Analysis	50
6	Nearshore Spectral Peak Frequency And Period Directional Spectral Propagation Analysis	51

Nomenclature

A	scale parameter	$[L^{1/3}]$
B	orthogonal spacing	$[L]$
B_0	deep water orthogonal spacing	$[L]$
C, C_1, C_2	wave celerity	$[L/T]$
C_g	wave group celerity	$[L/T]$
D	sediment diameter	$[L]$
d	water depth	$[L]$
E	wave energy per unit crest width	$[LF/L]$
f	wave frequency	$[1/T]$
f_{ij}	frequency of wave component ij	$[1/T]$
f_p	peak wave frequency	$[1/T]$
g	acceleration due to gravity	$[L/T^2]$
h	water depth	$[L]$
H	wave height	$[L]$
H_{mo}	significant wave height	$[L]$
K_r	refraction coefficient	$[-]$
K_s	shoaling coefficient	$[-]$
$K_r K_s$	combined refraction and shoaling coefficient	$[-]$
$(K_r K_s)_{eff}$	effective combined refraction and shoaling coefficient	$[-]$

k	wave number	[1/L]
L	wave length	[L]
L_o	deep water wave length	[L]
m_o	zero moment of wave spectrum	[L ²]
m_{oij}	zero moment of wave spectrum for section ij	[L ²]
m_1	first moment of wave spectrum with respect to either propagation direction or frequency	[L ² or L ² /T]
n	ratio of wave group celerity to wave celerity	[-]
S_{ds}	energy dissipation	[L ²]
S_{in}	wind input energy	[L ²]
S_{nl}	nonlinear wave-wave interaction energy	[L ²]
$S(f)$	frequency spectrum	[L ² T]
$S(f,\theta)$	directional wave spectrum	[L ² T]
$S(f_{ij},\theta_{ij})$	representative directional spectral energy density of wave component ij	[L ² T]
t	time	[T]
T	wave period	[T]
T_p	peak wave period	[T]
w	fall velocity	[L/T]
x, y	horizontal coordinate directions	[L]
y	distance offshore from the still water line	[L]

z	vertical coordinate direction	[L]
ΔE	relative energy of wave component	[-]
Δf	frequency band spacing	[1/T]
$\Delta \theta$	direction band spacing	[-]
α	Phillip's parameter	[-]
γ	specific weight spectral peak shape factor	[F/L ³] [-]
θ	wave propagation direction deviance from the mean direction	[-] [-]
θ_1, θ_2	wave propagation direction	[-]
θ_{ij}	representative direction of wave component ij	[-]
$\theta_{\max}, \theta_{\min}$	maximum and minimum deviations from the mean direction	[-]
θ_{mean}	mean spectral propagation direction	[-]
λ	JONSWAP shape parameter	[-]
σ	wave angular frequency frequency shape factor	[1/T] [-]
ϕ_o	three-dimensional complex velocity potential two-dimensional complex velocity potential	[L/T] [L/T]

ABSTRACT

Because of the importance of the effects of waves in nearshore coastal locations, it is necessary to have accurate and reliable nearshore wave information to depend upon for coastal design. Offshore wave data is often available for many coastal locations, but wave data in the nearshore is scarce. Usually, this offshore wave information is propagated into the nearshore through the implementation of a monochromatic analysis. A more accurate method for determining nearshore wave information may lie in the implementation of a directional spectral wave propagation analysis which includes variations in wave frequency and propagation direction. This type of analysis will better simulate wave propagation.

Two computer models developed by the U.S. Army Corps of Engineers are considered in this report. RCPWAVE is designed to perform a monochromatic wave propagation where STWAVE is designed to perform a directional spectral wave propagation. A third method, the component method, which performs directional spectral wave propagation with the use of RCPWAVE, will also be employed.

Conclusions from this investigation show the importance of considering the frequency/direction spread in a wave propagation analysis. With respect to a monochromatic propagation analysis, significantly different nearshore peak periods and nearshore mean propagation directions are generated by a directional spectral propagation analysis. It is concluded from the results obtained herein that one should

consider a directional spectral wave propagation method when entering into a coastal design problem.

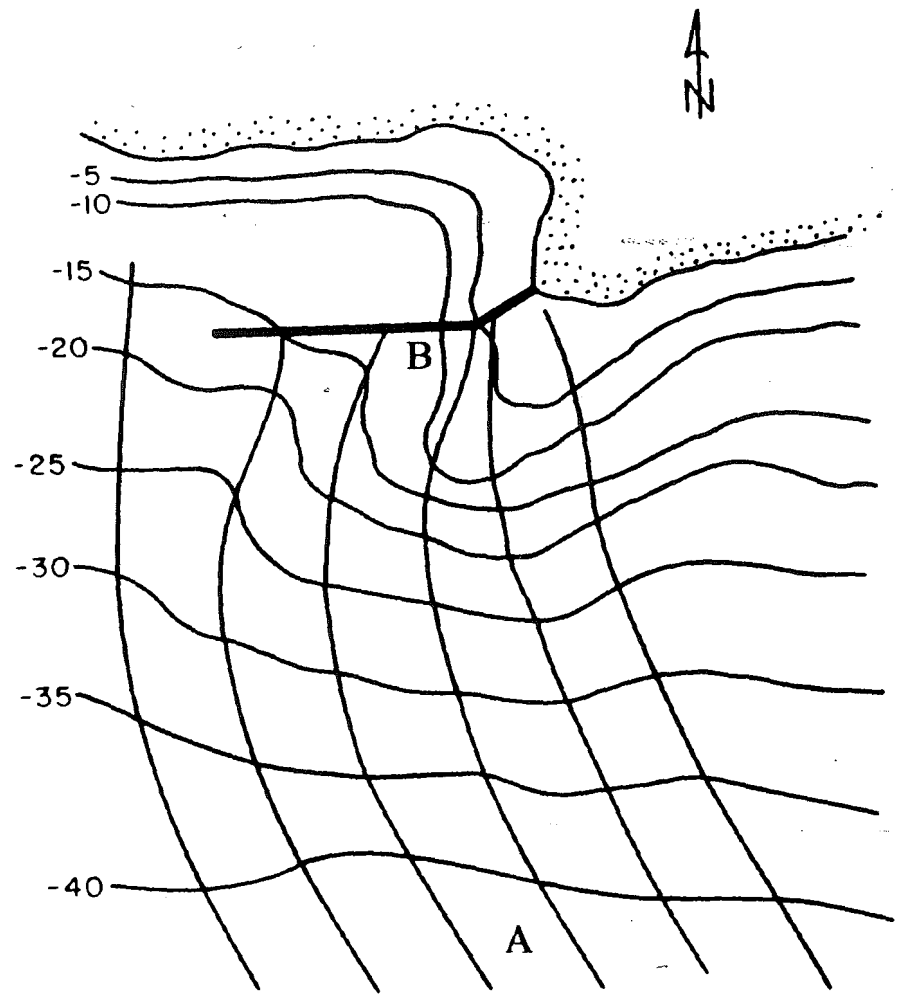
1.0 INTRODUCTION

1.1 Engineering Problem

An important concern for coastal design is determining the design wave conditions at the proposed structure location. A typical design wave is defined by a wave height, wave period, and wave propagation direction. Deep water wave conditions are usually readily available; however, the problem lies in transforming these deep water conditions as the waves propagate into the nearshore where coastal structures are located.

This basic design problem is illustrated in Figure 1.1 where point A indicates the deep water wave conditions and point B represents the nearshore conditions at the structure. The lines approaching the shoreline perpendicularly are wave orthogonals which indicate the refracted wave pattern for a monochromatic wave. The distance between these orthogonals is uniform in deep water, point A, but as they enter the nearshore, this spacing can increase or decrease as a function of the bathymetry. Refraction plus shoaling effects change the height and direction of individual waves as they approach the shore. Use of a single representative wave in this analysis will not likely produce results that are adequately representative of the nearshore transformation of a directional wave spectrum.

A - $(H_s, T_p, \theta_d)_o$
B - $(H_s, T_p, \theta_d)_n$



4

Figure 1.1 Basic Design Problem Definition (Sorensen (1993))

1.2 Scope of Investigation

Presently, the most common method for obtaining nearshore wave conditions is through the implementation of a monochromatic wave propagation analysis. A monochromatic analysis uses one representative wave condition and moves this wave across the site bathymetry into the nearshore. In a true coastal environment, the wave conditions entering a site are not simply defined by one wave height, one wave period, and one wave direction, but are composed of a directional spectrum of waves covering a range of frequencies and directions. An example of such a wave condition is given in Figure 1.2. This shows the spectral energy, $S(f,\theta)$, versus both frequency and propagation direction. This wave spectrum was obtained from a U.S. Army Corps of Engineers operated directional wave gage array located in Duck, North Carolina. The spectral peak is representative of the spectral peak period and propagation direction.

The scope of this investigation is to compare the resulting nearshore wave conditions from a monochromatic wave propagation with those from a directional spectral wave propagation to discover the impact of neglecting variations in frequency and propagation direction. Specifically, this investigation will include a comparison between monochromatic propagation versus directional spectral propagation as it relates to wave height, wave propagation direction, and wave period at the nearshore location. The analysis of these wave conditions will include the effects of refraction, shoaling, and diffraction.

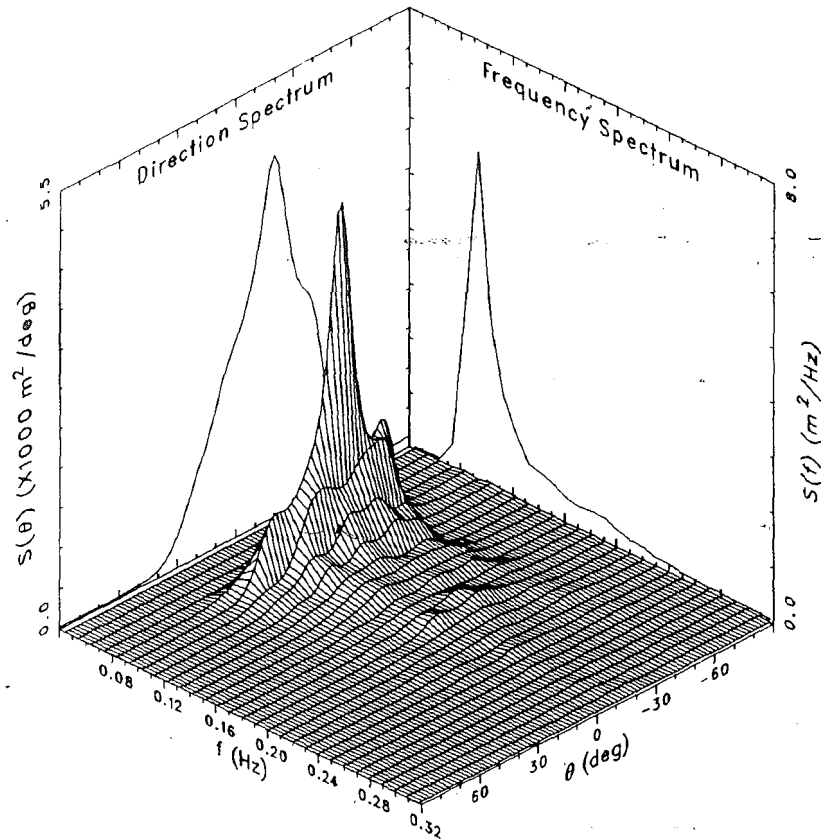


Figure 1.2 Directional Spectrum, Courtesy of the U.S. Army Corps of Engineers Field Research Facility, Duck, NC

1.3 General Wave Theory Concepts

This section contains a summary of selected wave theory concepts required as background to the material presented in this thesis. For further discussion of these concepts see Dean and Dalrymple (1984) and Sorensen (1993).

When neglecting changes due to bottom and surface effects, such as wind and bottom friction, as well as wave reflection, the change in height and direction of a wave as it moves into the nearshore are caused by three mechanisms: refraction, shoaling, and diffraction. Wave refraction is due to variations in wave celerity along the wave crest: because of this variation, the wave will refract toward areas of lower celerity. This concept can be further clarified by giving its relation to wave energy. Equation 1.1 shows that the wave energy per unit crest width is directly a function of the wave height squared.

$$E = \frac{\gamma H^2 L}{8} \quad (1.1)$$

where:

E	wave energy per unit crest width
γ	specific weight
H	wave height
L	wave length

In Figure 1.1, The wave orthogonals have a constant deep water spacing, B_0 . As the wave propagates into the nearshore, these orthogonals bend, or refract, as a result of the local bathymetry, and the energy density between these orthogonals increases or decreases owing to a convergence or divergence in the wave orthogonal paths.

Introducing Equation 1.2, it is therefore possible to relate this orthogonal spacing with wave refraction, by a refraction coefficient defined as:

$$K_r = \sqrt{\frac{B_o}{B}} \quad (1.2)$$

where:

K_r	refraction coefficient
B_o	deep water orthogonal spacing
B	orthogonal spacing

A refraction coefficient greater than 1 is indicative of a convergence of energy and an increase in wave height at the nearshore location; whereas a value less than 1 is indicative of a divergence in energy and a decrease in wave height.

Wave shoaling is directly a function of the relative depth: the water depth over the wave length (d/L). As a wave moves into the nearshore, it begins to feel bottom, or shoal. Equation 1.3 defines the shoaling coefficient, K_s , which is an indicator of the change in wave height caused by shoaling.

$$K_s = \sqrt{\frac{L_o}{2nL}} \quad (1.3)$$

where:

K_s	shoaling coefficient
L_o	deep water wave length
n	ratio between wave group celerity and wave celerity

Combining the effects of both wave refraction and wave shoaling in Equation 1.4, the wave height at the nearshore location can be determined.

$$\frac{H}{H_0} = K_r K_s \quad (1.4)$$

In Equation 1.4, H_0 represents the deep water wave height and $K_r K_s$ is called the combined refraction and shoaling coefficient.

Because there are areas of energy convergence and divergence along the nearshore wave crest as a result of refraction, there is a tendency for this energy to move along the wave crest to achieve a uniform energy spread. This energy transfer along the wave crest is known as wave diffraction caused by local bathymetry. Wave diffraction allows the wave to approach a constant wave height along its crest. To combine the effects of wave diffraction with those from wave refraction, a solution must be developed for the three-dimensional Laplace equation:

$$\frac{\partial^2 \phi_o}{\partial x^2} + \frac{\partial^2 \phi_o}{\partial y^2} + \frac{\partial^2 \phi_o}{\partial z^2} = 0 \quad (1.5)$$

where:

ϕ_o	three-dimensional complex velocity potential
x, y	horizontal coordinate directions
z	vertical coordinate direction

In order to obtain a solution to Equation 1.5, boundary conditions including bottom, surface, and lateral conditions must be implemented.

2.0 NUMERICAL APPROACH

Two numerical models developed by the U.S. Army Corps of Engineers are considered for use in the comparison of monochromatic wave propagation, RCPWAVE, versus directional spectral wave propagation, STWAVE. The following sections briefly describe these models. Please refer to the Coastal Modeling System (CMS) User's Manual (Cialone et al. (1992)) if a more detailed explanation is desired. A third numerical approach, a component analysis, will be discussed for use in the analysis of directional spectral wave propagation.

2.1 RCPWAVE

The Regional Coastal Processes Wave Propagation Model (RCPWAVE) is a finite difference based computer model which simulates monochromatic, linear wave propagation. This model may be used to generate a first-order analysis of wave characteristics as they change when propagating over variable coastal bathymetry.

2.1.1 Model Theory

RCPWAVE applies both the mild slope equation, Berkhoff (1972), and the conservation of waves equation, which may be found in Dean and Dalrymple (1984). The mild slope equation, given in Equation 2.1, is based upon an irrotational, linear, simple harmonic wave system and is applicable from deep water up to the breaker zone.

$$\frac{\partial}{\partial x} [CC_g \frac{\partial \phi_o}{\partial x}] + \frac{\partial}{\partial y} [CC_g \frac{\partial \phi_o}{\partial y}] + \sigma_2 \frac{C_g}{C} \phi_o = 0 \quad (2.1)$$

where:

C	wave celerity
C_g	wave group celerity
ϕ_o	two-dimensional complex velocity potential
σ	wave angular frequency ($2\pi/T$)
T	wave period

The equation includes not only refraction and shoaling but also diffraction resulting from the local bathymetry by employing a two-dimensional form of Equation 1.5 along with a bottom boundary condition to be integrated over water depth. RCPWAVE does not include diffraction as a result of coastal structures. The two-dimensional complex velocity potential is a function of wave height and can thus be related to the combined refraction and shoaling coefficient via Equation 1.4.

The conservation of waves equation, given in Equation 2.2, expresses the wave irrotationality and balances the number of waves coming into a horizontal space, defined by x and y, with the number of waves exiting the same horizontal space.

$$\frac{\partial(k \sin\theta)}{\partial x} - \frac{\partial(k \cos\theta)}{\partial y} = 0 \quad (2.2)$$

where:

k wave number where:

$$\sigma^2 = gk \tanh(kd)$$

g acceleration due to gravity
 d water depth

θ wave propagation direction as defined in Figure 2.1

Because the scope of the project only includes the use of RCPWAVE in the analysis of wave propagation outside of the surf zone, the methods employed in the model for wave propagation within the surf zone will not be discussed.

2.1.2 Model Assumptions

The model's most limiting factor lies in its assumption of a linear, monochromatic, short wave system. This assumption allows the model to simulate steady state wave propagation including the effects of refraction, diffraction, and shoaling resulting from the site bathymetry. RCPWAVE neglects wave reflection outside of the surf zone.

2.1.3 Input Requirements

RCPWAVE requires the user to provide deep-water wave conditions including wave height, period, and propagation direction. In addition, the user needs to provide detailed site bathymetry.

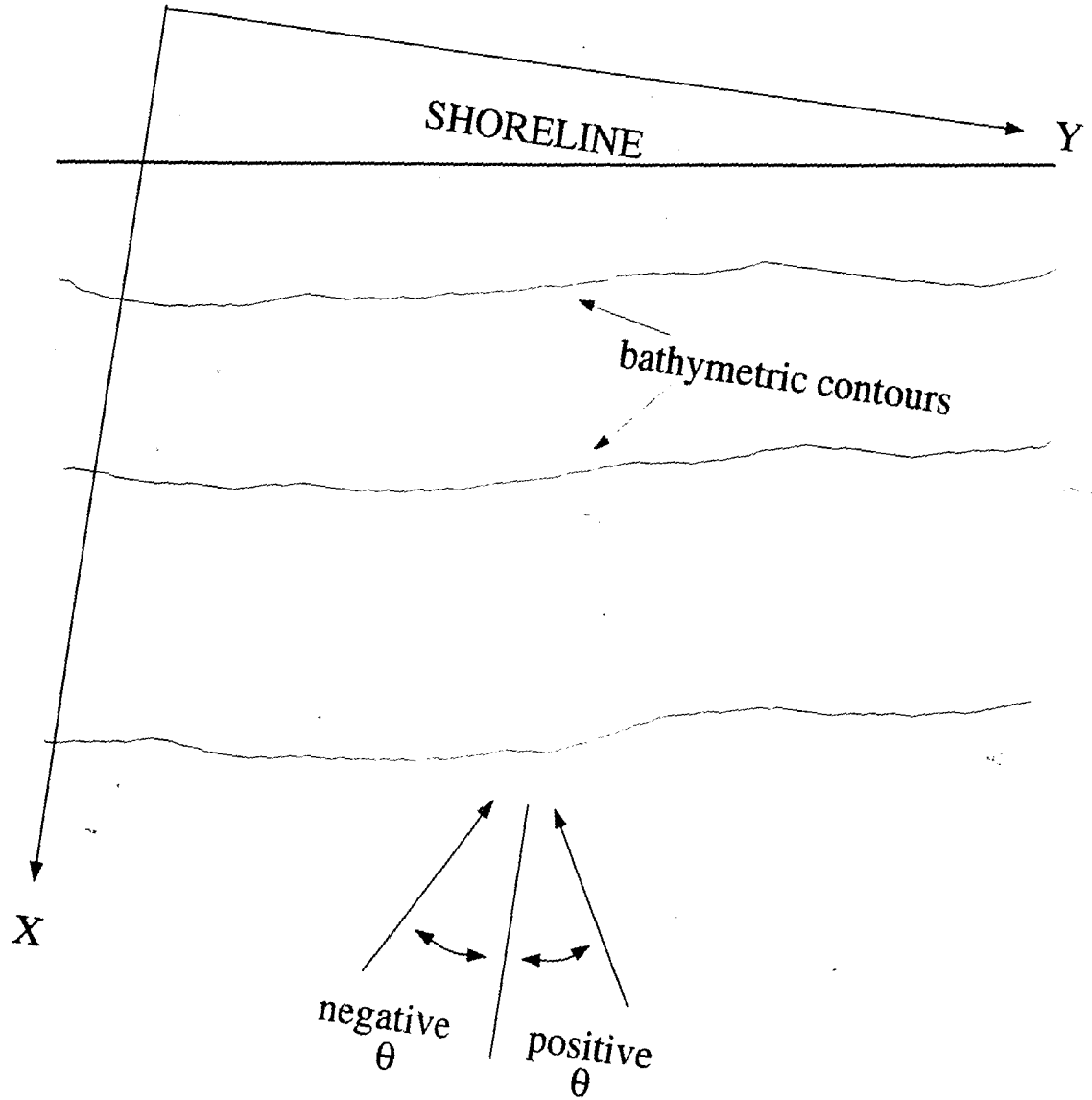


Figure 2.1 Definition of Wave Propagation Direction, θ (Cialone et al. (1992))

2.1.4 Model Computation

Using a finite difference method through a computational grid similar to that shown in Figure 2.2, RCPWAVE is able to generate solutions to Equations 2.1 and 2.2. Using the deep water wave conditions, the model first generates initial estimates of both the wave and wave group celerities, wave angle, and wave height for all computational grid points. Because they are directly a function of the wave number and wave period, the initial estimates for the wave and wave group celerities are obtained by employing the definition of the wave number stated previously. The initial guess for the wave angle is calculated from Snell's Law:

$$\frac{\sin\theta_1}{C_1} = \frac{\sin\theta_2}{C_2} \quad (2.3)$$

where:

θ_1, θ_2	wave propagation directions at locations 1 and 2
C_1, C_2	wave celerity at locations 1 and 2

Snell's law gives a relationship between the deep water approach angle and celerity and the nearshore approach angle and celerity if the bottom contours are shore parallel. First estimates of the wave height are obtained from the product of the deep water wave height, the refraction coefficient, and the shoaling coefficient, where the refraction and shoaling coefficients are based upon the initial estimates of the wave number and the approach angle. The final values of these parameters are then solved

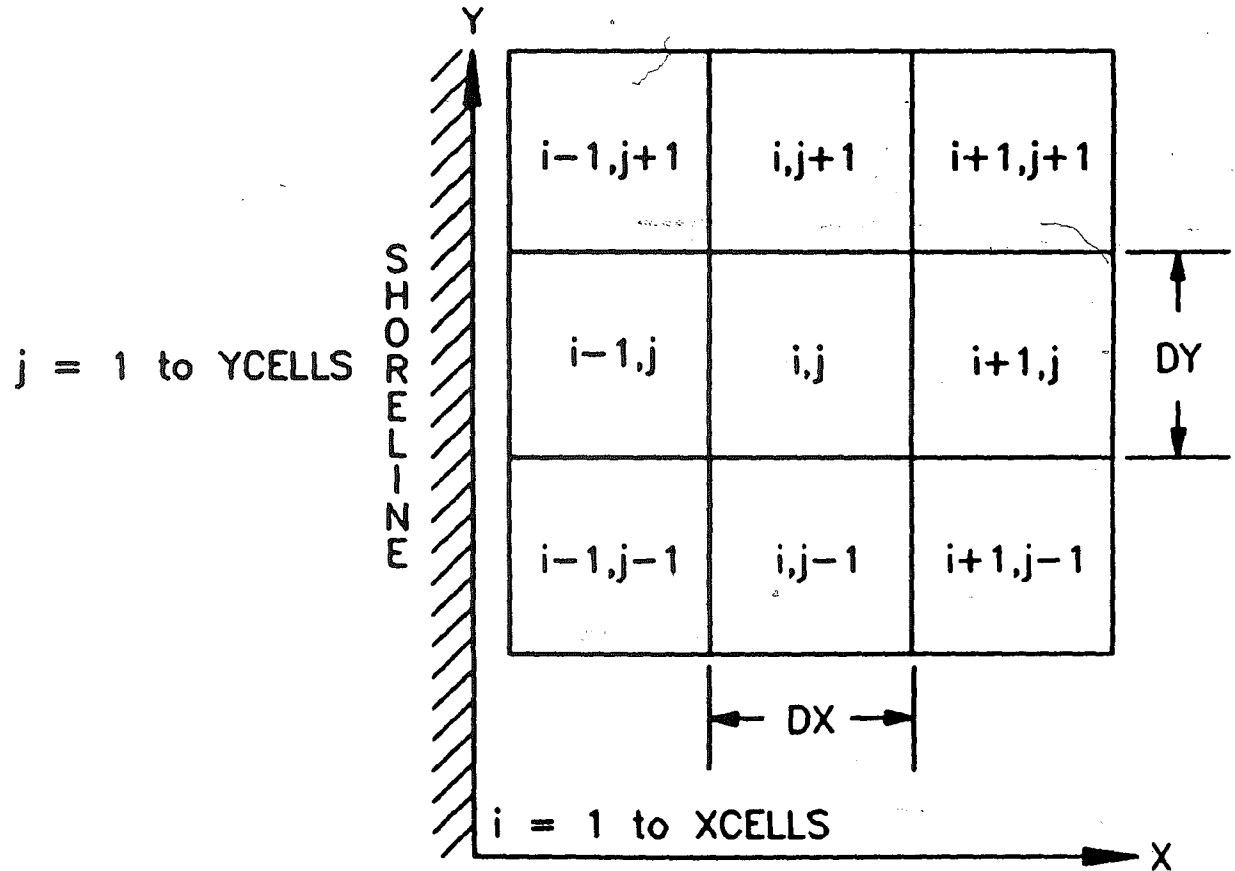


Figure 2.2 RCPWAVE Computational Grid (Cialone et al. (1992))

for through an iterative finite difference process. After a solution has been found for all computational grid points along the offshore row, RCPWAVE repeats the procedure for the next consecutive row. This continues until the model has generated results for each computational point.

2.1.5 Generated Output

The output produced by RCPWAVE includes the following:

- wave height
- wave propagation direction
- wave number

The model will generate any of these quantities, with a two decimal place accuracy, for any specified block of computational grid cells. The combined refraction and shoaling coefficient can then be calculated from the given deep water wave height and calculated nearshore wave height using Equation 1.4.

2.2 STWAVE

STWAVE is a finite-difference computer model applied on a computational grid to simulate spectral wave energy propagation through the nearshore. The model may be used to analyze directional wave energy spectra propagation.

2.2.1 Model Theory

The model is based on the spectral energy balance equation given in Equation 2.4, where each energy term represents a change in energy density, or energy per unit surface area, with respect to time without including the specific weight term (see Sorensen (1993)).

$$S_{in} + S_{nl} + S_{ds} = \frac{\partial S(f, \theta)}{\partial t} + C_g \cdot \nabla S(f, \theta) \quad (2.4)$$

where:

S_{in}	wind input energy
S_{nl}	nonlinear wave-wave interaction energy transfer
S_{ds}	energy dissipation by wind and bottom friction
$S(f, \theta)$	directional wave spectrum where:

$$S(f, \theta) df d\theta = \sum_f^{f+\Delta f} \sum_\theta^{\theta+\Delta\theta} \frac{H^2}{8}$$

f	wave frequency
θ	deviance from the mean direction as defined in Figure 2.3
t	time
∇	differential operator:

$$\frac{\partial}{\partial x} \bar{i} + \frac{\partial}{\partial y} \bar{j}$$

In essence, the spectral energy balance equation calculates wave growth and change in spectral energy with both time and space.

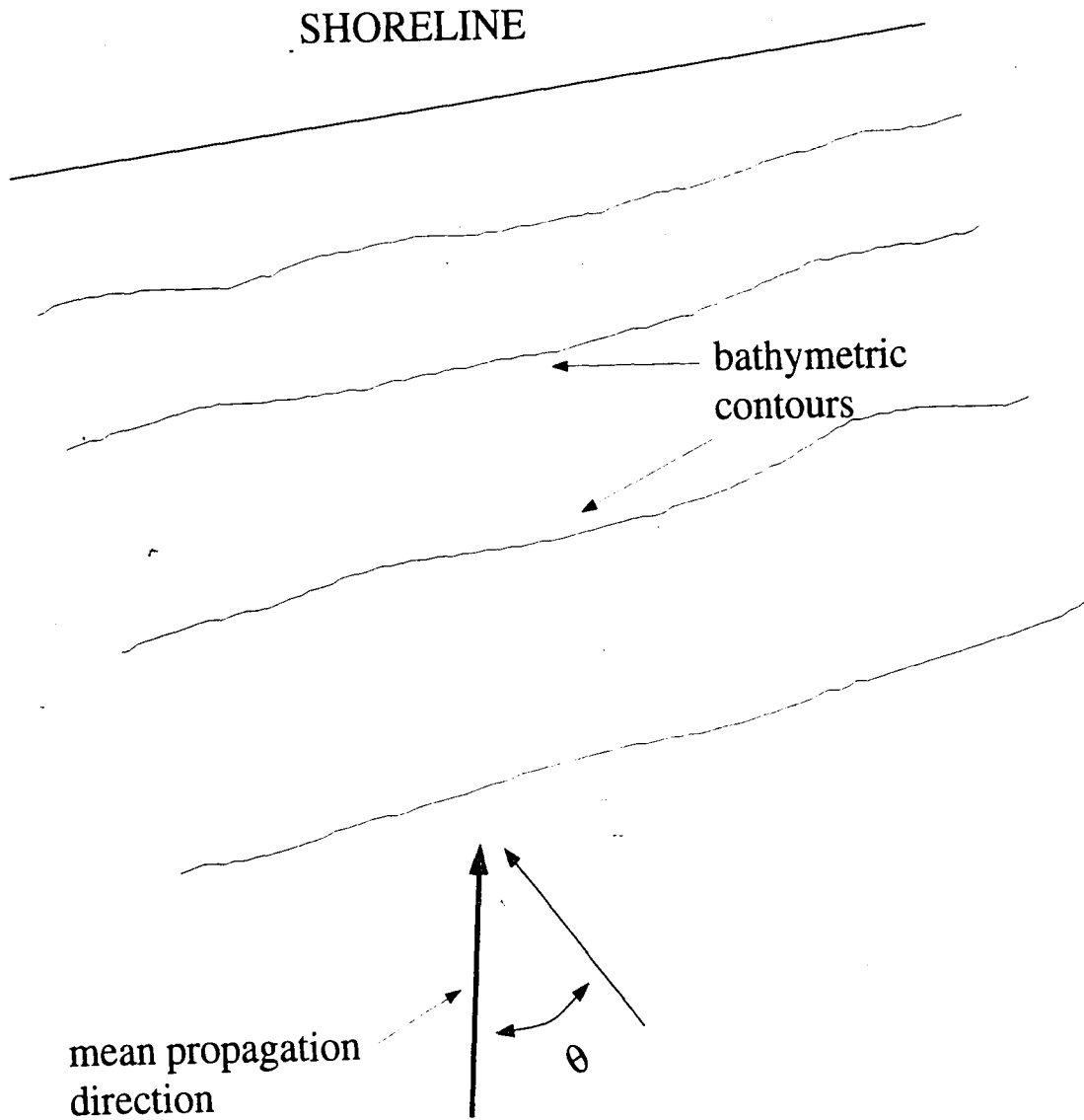


Figure 2.3 Definition of Deviance From Mean Propagation Direction, θ

2.2.2 Model Assumptions

Many of the terms in the spectral energy balance equation are eliminated due to the assumptions made to simplify STWAVE for efficiency. The following is a list of these assumptions:

1. only wave energy directed into the computational grid is of importance; therefore, wave energy directed out of the grid is neglected.
2. time variation of wave energy at any point in the computational grid is so slow that when compared with the required time for wave propagation through the grid, this energy change is negligible.
3. the model neglects the wave generation, nonlinear transfer, and dissipation terms.

Assumption 3 implies that there is no wave growth or decay within the computational grid; therefore, the left hand side of Equation 2.3 is zero. Also, Assumption 2 indicates that there is no time variation in wave energy within the computational grid allowing the first term on the right hand side of Equation 2.4 to equal zero. The reduced version of the spectral energy balance equation solved in STWAVE is:

$$C_g \cdot \nabla S(f, \theta) = 0 \quad (2.5)$$

Equation 2.5 indicates that any spectral energy change in one coordinate direction is equally balanced by a change in the other coordinate direction so as to allow the net change to be zero.

2.2.3 Model Computation

STWAVE requires wave characteristics and bottom bathymetry as input. The model allows much flexibility in the input format of the wave characteristics and allows the bathymetry to be either constant or variable.

To meet the model assumptions, the computational grid used must be small enough that wave propagation through the grid will occur in 30 minutes or less. STWAVE assigns the offshore column of the grid with the input boundary condition spectrum and then generates new spectral information along each consecutive column within the grid by including energy changes due to shoaling and refraction between each column.

As Figure 2.4 indicates, the directional spectrum at each grid point is divided into components through the use of frequency and direction bands. In Figure 2.4, each semicircular ring is a frequency band and each pie shape delineated by approach directions is a direction band. Each component is then propagated separately to the next column by employing finite difference operations to the spectral energy balance equation. When all frequency direction components from one column are propagated through to the next column, they are recombined to form a directional spectrum at each grid point along the new column. After the spectral information of a column is complete, STWAVE analyzes the column for wave breaking.¹ If it is determined that breaking occurs, the energy which is lost during breaking is removed from the spectrum; therefore limiting the energy in the new spectrum generated in the consecutive columns (Davis et al. (1991)).

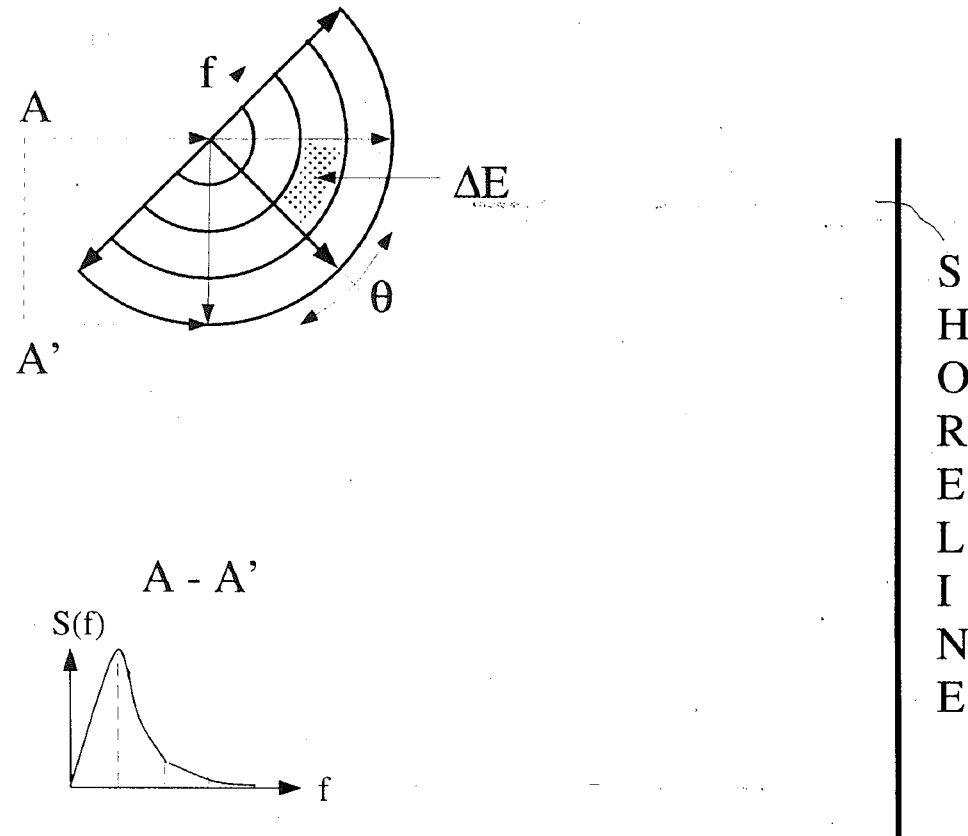


Figure 2.4 Frequency and Direction Bands for Directional Spectral Analysis

The following output is produced by STWAVE for each desired point within the computational grid:

- energy based significant wave height
- spectral peak period
- mean spectral propagation direction
- wave frequency spectrum
- wave frequency-direction spectrum

Using the significant wave height for the nearshore point, a combined refraction and shoaling coefficient is determined from Equation 1.4.

2.2.4 Model Operation

In the attempt to use STWAVE for directional spectral wave propagation, problems were encountered. The generated output yielded unreasonable results. After acquiring assistance from the Coastal Engineering Research Center of the U.S. Army Corps of Engineers, it was concluded that the problems could not be resolved without an extensive effort and; therefore, STWAVE will not be used further in this investigation. The U.S. Army Corps of Engineers is currently improving STWAVE, and when the program proves to be user-friendly, it could become state-of-the-art for spectral wave propagation analysis.

2.3 Component Analysis

The component analysis generates an effective combined refraction and shoaling coefficient of a transformed directional spectrum by dividing it into a number

of frequency/direction components as depicted in Figure 2.4. Each component is then propagated across the bathymetric grid to produce a representative refraction and shoaling coefficient owing to propagation across the grid. The results can then be combined to yield the resulting transformed directional spectrum.

2.3.1 Theory

The component analysis is modeled after Goda (1985) where the resulting refraction and shoaling coefficient is given by the following equation:

$$(K_r K_s)_{eff} = \sqrt{\frac{1}{m_0} \int_0^\infty \int_{\theta_{min}}^{\theta_{max}} S(f, \theta) K_r^2(f, \theta) K_s^2(f) d\theta df} \quad (2.6)$$

where:

$(K_r K_s)_{eff}$	effective combined refraction and shoaling coefficient
$\theta_{min}, \theta_{max}$	maximum and minimum deviations from the mean direction of wave propagation
m_0	zero moment of wave spectrum

Equation 2.6 is derived from Equation 1.4 where the wave height is found using the definition of the directional spectral energy density function. The directional spectral energy density serves as a weighting parameter by giving more emphasis to the combined refraction and shoaling coefficients generated near the spectral peak wave conditions and less weight with further deviation from these conditions. Reviewing the relationship between the refraction and shoaling coefficient and the wave height, Equation 1.4, as well as the definition of wave energy, Equation 1.1, it is necessary

to use the square of the directional spectral energy function as the weighting function so as to be representative of the wave height.

Simplifying Equation 2.6 by using summation operations yields the following:

$$(K_r K_s)_{eff} = \sqrt{\sum_{i=1}^M \sum_{j=1}^N (\Delta E)_{ij} (K_r K_s)_{ij}^2} \quad (2.7)$$

and

$$\Delta E = \frac{m_{oij} \int_{\Delta f} \int_{\Delta \theta} S(f, \theta) d\theta df}{m_o \int_{f_{min}}^{f_{max}} \int_{\theta_{min}}^{\theta_{max}} S(f, \theta) d\theta df} \quad (2.8)$$

where:

ΔE relative energy of the wave component
 m_{oij} zero moment of wave spectrum for section ij

This form allows the directional spectrum to be divided into components, each representing an incremental change in spectral energy, frequency, and direction.

2.3.2 Computation

To apply the component method of determining combined refraction and shoaling to a directional spectrum, the spectrum needs to be divided into segments by the use of frequency and direction bands with spacings Δf and $\Delta \theta$, respectively, as depicted in Figure 2.4.

Each segment is represented by a specific frequency and specific direction that can be used as input into RCPWAVE. The representative frequency, f_{ij} , is taken as the frequency at the centroid of the representative energy volume; whereas, the representative direction, θ_{ij} , is approximated as the direction at the center of the direction increment, $\Delta\theta$. This is illustrated in Figure 2.5.

The relative energy for each wave component is the ratio between the volume under the spectral energy density surface with respect to the frequency and direction increments and the total volume under the spectral surface. It is computed by integrating over both frequency and direction as shown in Equation 2.7.

The nearshore spectral peak period and mean spectral propagation direction is obtained by recombining the directional spectrum and finding the first moment of the wave spectrum, m_1 , with respect to frequency and to propagation direction. Equation 2.9 illustrates this for the determination of the nearshore mean spectral propagation direction, θ_{mean} .

$$\theta_{mean} = \frac{m_1}{m_0} = \frac{\int_{f_{min}}^{f_{max}} \int_{\theta_{min}}^{\theta_{max}} \theta S(f,\theta) df d\theta}{\int_{f_{min}}^{f_{max}} \int_{\theta_{min}}^{\theta_{max}} S(f,\theta) df d\theta} \quad (2.9)$$

Using the nearshore directional spectral energy density, Equation 2.9 gives the nearshore mean propagation direction based on the centroid of the energy distribution.

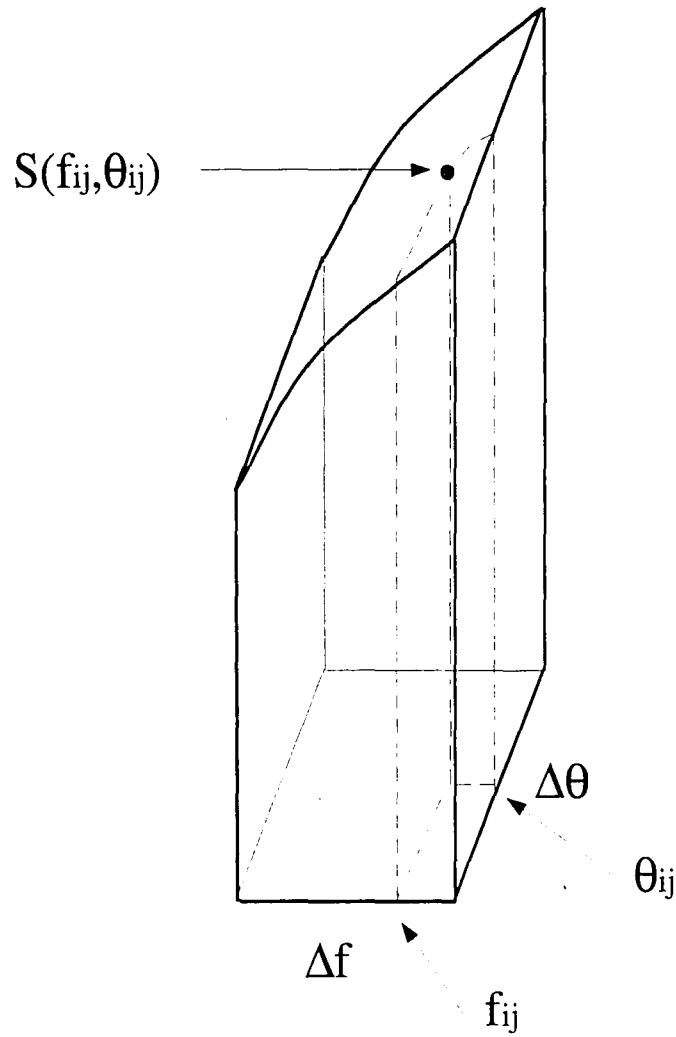


Figure 2.5 Definition of Representative Frequency and Direction, f_{ij} and θ_{ij}

For ease of computation, Equation 2.9 is approximated with summations in Equation 2.10.

$$\theta_{mean} = \frac{\sum_{i=1}^M \sum_{j=1}^N \theta_j \frac{H_{ij}^2}{8} \Delta f_{ij} \Delta \theta_{ij}}{\sum_{i=1}^M \sum_{j=1}^N \frac{H_{ij}^2}{8} \Delta f_{ij} \Delta \theta_{ij}} \quad (2.10)$$

The wave heights and propagation directions for each wave component entered into Equation 2.10 are obtained from the RCPWAVE output. A similar method is employed for generating the nearshore spectral peak wave period.

2.3.3 STWAVE Comparison

There are several similarities between the component analysis and STWAVE. Both divide the deep water input directional spectrum into segments by introducing frequency and direction bands, both include refraction and shoaling effects as the component is propagated into the nearshore, and both recombine the segments to give a combined refraction and shoaling coefficient representative of the nearshore directional spectrum.

There are two fundamental differences between the two approaches. Firstly, STWAVE performs a bookkeeping operation as the component is moved from column to column, but the component analysis only recombines the components when the nearshore point of interest is reached. The method employed by STWAVE may yield

a more accurate solution; however the level of this higher accuracy can be deemed insignificant.

The second difference lies in the treatment of bottom induced wave diffraction. The component method employs the mild slope equation to each spectral component as it is propagated to the next grid cell. This procedure concurrently solves for wave refraction and wave diffraction. In contrast to the component method, as each spectral energy component in STWAVE is propagated to the next grid cell, it is modified to include the effects of shoaling and pure refraction only. After the energy component has been moved it is adjusted to include bottom wave diffraction effects.

3.0 MODEL EXPERIMENT

In order to compare monochromatic wave propagation versus directional spectral wave propagation, a fundamental test site is simulated based upon empirical beach profile equations developed through field studies. The wave conditions analyzed are chosen such as to represent typical design wave conditions. The following sections detail the experiment hydrography and wave conditions.

3.1 Hydrography

To simplify the hypothetical experiment site, the bottom hydrography is generalized to eliminate effects from local bathymetric characteristics. The experiment site bathymetry is based on an empirical beach profile first introduced by Bruun (1954) and stated in Equation 3.1 (see Work (1991)).

$$h(y) = Ay^{2/3} \quad (3.1)$$

y distance offshore from the still water line
 $h(y)$ water depth at y with respect to the mean water line
 A scale parameter

The scale parameter in Equation 3.1 is dependent on sediment grain size. Based on numerous beach profiles, Dean (1987) and Moore (1982) developed the relationship, given in Figure 3.1, between both the sediment size or fall velocity and the scale parameter.

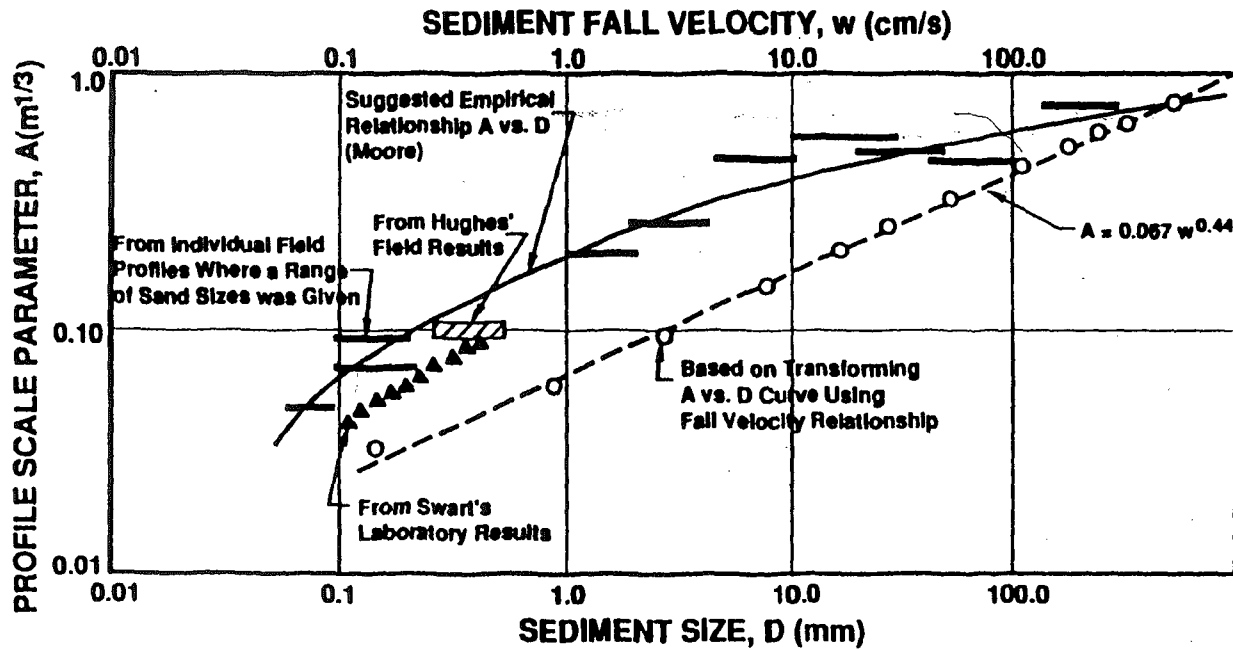


Figure 3.1 Beach Profile Factor, A , Versus Sediment Diameter, D , and Fall Velocity, w [Dean (1987); modified from Moore (1982)]

Using a sediment diameter, D , of 0.5 mm yields a scale parameter, A , equal to $0.125 \text{ m}^{1/3}$. The generated beach profile extends from deep water into a 5 meter water depth and is given in Figure 3.2. The bathymetry is held constant with respect to the longshore direction so as to provide uniform hydrography through the implementation of shore parallel contours.

3.2 Wave Conditions

Wave conditions are chosen so as to cover a range of frequencies and mean propagation directions. Because the investigation is independent of the deep water wave height, this is chosen as 1 meter for easy computation.

The wave conditions that will be analyzed are tabulated below:

DEEP WATER WAVE CONDITIONS										
CASE NUMBER	1	2	3	4	5	6	7	8	9	10
MEAN DIRECTION (deg)	0	15	30	45	60	0	15	30	45	60
PERIOD (sec)	7	7	7	7	7	12	12	12	12	12
FREQUENCY (Hz)	0.14	0.14	0.14	0.14	0.14	0.08	0.08	0.08	0.08	0.08

Table 1

BEACH PROFILE

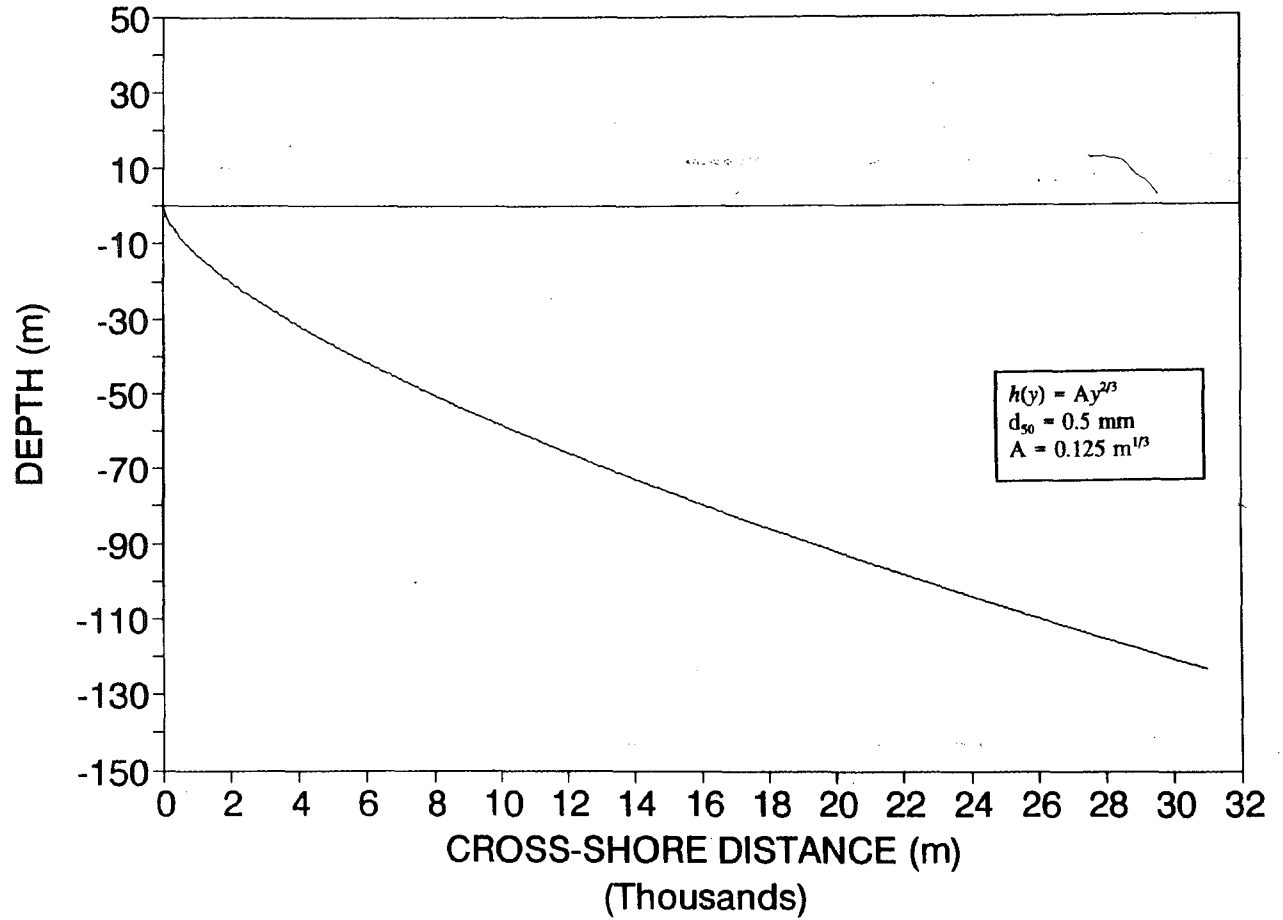


Figure 3.2 Hypothetical Experiment Site Bathymetry

4.0 MONOCHROMATIC WAVE ANALYSIS

4.1 Conditions Analyzed

The wave conditions analyzed in this portion of the investigation are represented by the deep water wave characteristics given in Table 1. These wave characteristics each represent a different monochromatic wave system to be used in analyzing monochromatic wave propagation.

4.2 RCPWAVE Analysis

Each set of deep water wave conditions, including wave height, wave period, and wave propagation direction, is input directly into RCPWAVE. The model then propagates the monochromatic wave through the test site bathymetry until the 5 meter water depth is reached. At the nearshore 5 meter water depth, RCPWAVE generates a wave height from which a combined refraction and shoaling coefficient is calculated using Equation 1.4.

4.3 Results

For the ten test monochromatic wave conditions, RCPWAVE yields the combined refraction and shoaling coefficients tabulated in Table 2.

COMBINED REFRACTION AND SHOALING COEFFICIENT - $K_r K_s$ Monochromatic Propagation Analysis		
Deep Water Propagation Direction (deg)	Deep Water $T_p = 7$ seconds	Deep Water $T_p = 12$ seconds
0	0.91	1.00
15	0.91	0.99
30	0.89	0.95
45	0.86	0.88
60	0.78	0.76

Table 2

For monochromatic wave propagation, the wave period remains constant as the wave moves into the nearshore; therefore, the nearshore wave periods for the test conditions are 7 seconds and 12 seconds. As the monochromatic wave system propagates into the nearshore, refraction effects cause it to bend, yielding a new propagation direction. The nearshore propagation direction for each test wave condition is given in Table 3.

NEARSHORE PROPAGATION DIRECTION (deg) Monochromatic Propagation Analysis		
Deep Water Propagation Direction (deg)	Deep Water $T_p = 7$ seconds	Deep Water $T_p = 12$ seconds
0	0	0
15	13	8
30	25	16
45	37	24
60	47	29

Table 3

5.0 DIRECTIONAL SPECTRAL ANALYSIS

5.1 Conditions Analyzed

The wave conditions used in this section of the analysis are given in the form of a directional spectrum, represented by a spectral energy density function. The spectral peak wave conditions represented by these spectra are given in Table 1. Using these significant conditions, directional spectra are generated through the use of a spectral model: details of this modelling follow.

5.2 Directional Spectrum Generation

In order to analyze directional spectral wave propagation versus monochromatic wave propagation, a directional system with wave conditions equivalent to those of the monochromatic system must be developed. By implementing a frequency spectral model along with significant wave characteristics, this goal can be achieved. The following sections outline the chosen spectral model and how it is modified to represent a directional system.

5.2.1 Frequency Spectrum

A JONSWAP (Joint North Sea Wave Program) one-dimensional spectra model is utilized in the generation of a directional frequency spectrum. The JONSWAP spectrum is defined below:

$$S(f) = \frac{\alpha g^2}{(2\pi)^4 f^5} e^{-1.25(f/f_p)^4} \gamma e^{-((f-f_p)^2 / 2\sigma^2 f_p^2)} \quad (5.1)$$

where:

S(f)	frequency spectrum energy density
f_p	peak frequency
α	Phillip's parameter
γ	spectral peak shape factor
σ	frequency shape factor

In Equation 5.1, a recommended value of 3.3 is used for the spectral peak shape factor, γ , and the frequency shape factor has values as follows:

$$\begin{aligned} \sigma &= 0.07 && \text{when } f < f_p \\ \sigma &= 0.09 && \text{when } f > f_p \end{aligned}$$

The Phillip's parameter, α , is based on the following equation developed by Mitsuyasu (1980):

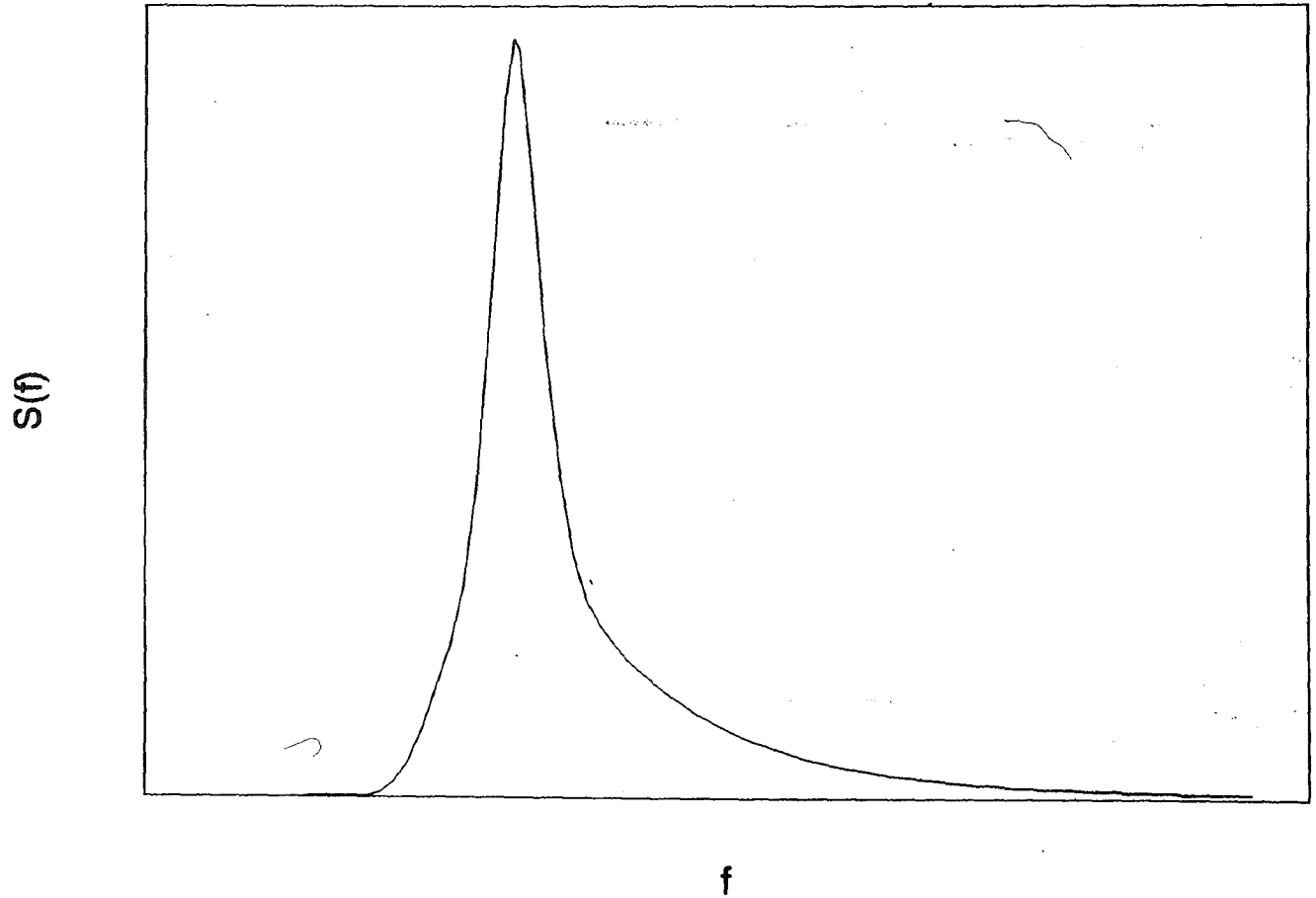
$$H_{mo} = 4g(\alpha\lambda)^{1/2} f_p^{-2} \quad (5.2)$$

where:

H_{mo}	significant wave height
λ	JONSWAP shape parameter

Equation 5.2 allows the JONSWAP spectrum to be plotted for a selected significant wave height. The JONSWAP shape parameter is taken to be 1.96E-4 when calculated from the JONSWAP model taking the spectral peak shape factor and frequency shape factor values as defined above (see Tucker (1991)). The JONSWAP spectra model gives a spectral energy density distribution with respect to frequency similar to that in Figure 5.1.

JONSWAP SPECTRUM



38

Figure 5.1 JONSWAP One-dimensional Spectra Model Distribution

To apply the JONSWAP spectrum, upper and lower cutoff frequencies are employed. The recommended values of 0.3 and 3.0 times the peak frequency are used. The generated one-dimensional frequency spectra for the 7 and 12 second peak period systems are given in Figures 5.2 and 5.3.

5.2.2 Directional Spread

In the creation of a directional spectrum, the frequency spectrum must be varied with respect to deviation from the mean propagation direction. The JONSWAP spectrum can be spread directionally by introducing a directional spreading function:

$$S(f,\theta) = S(f) G(f,\theta) \quad (5.3)$$

where:

$G(f,\theta)$ directional spreading function
defined so:

$$\int G(f,\theta) df d\theta = 1$$

Two directional spreading functions are considered for this investigation: the 'cosine squared' function and the Mitsuyasu (1975) function.

The cosine squared directional spreading function is solely dependent on the deviance from the mean propagation direction making it straight forward in application. It is given by:

JONSWAP SPECTRUM

7 SECOND PERIOD

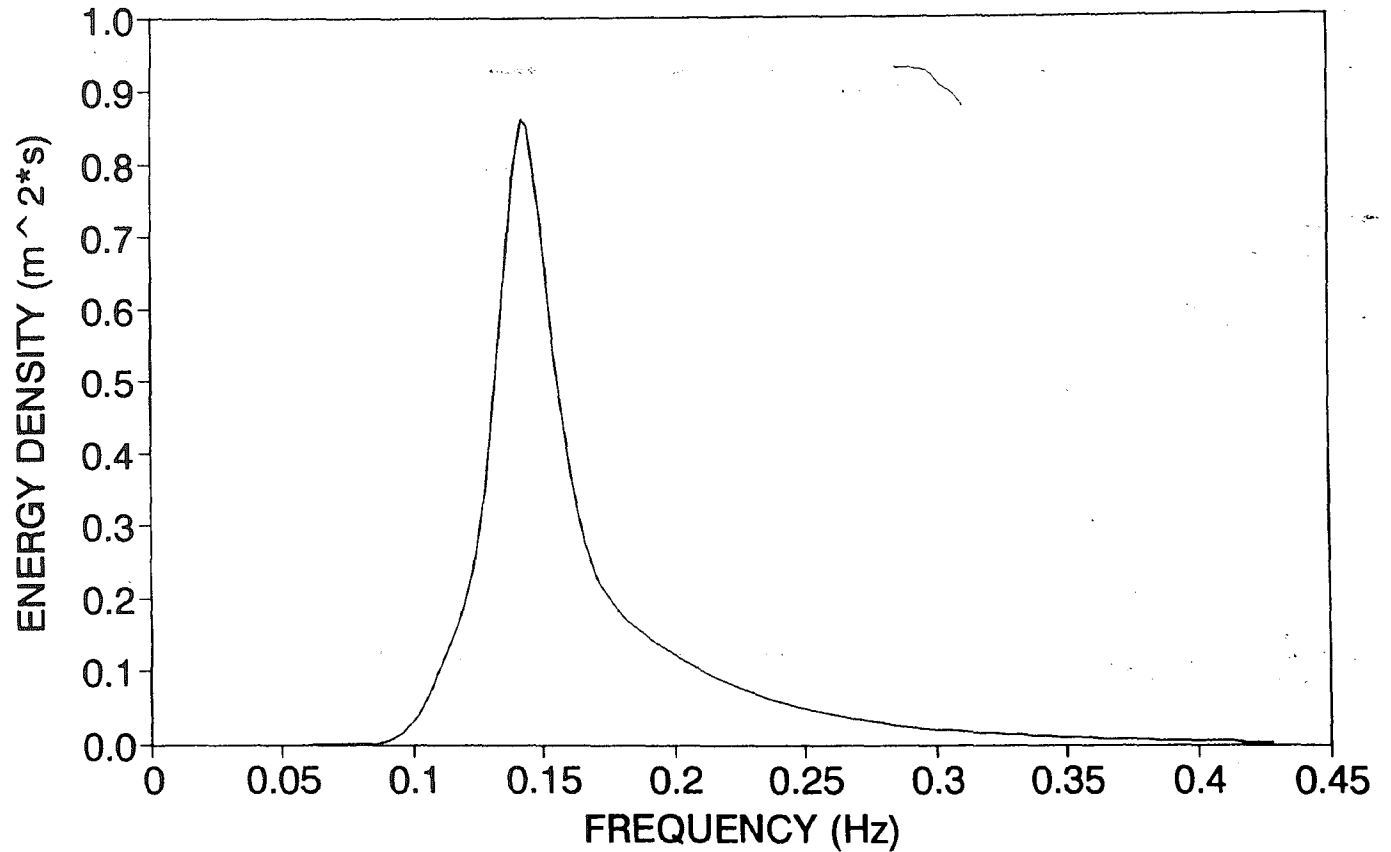


Figure 5.2 JONSWAP Frequency Spectrum: Deep Water Wave Period - 7 seconds

JONSWAP SPECTRUM

12 SECOND PERIOD

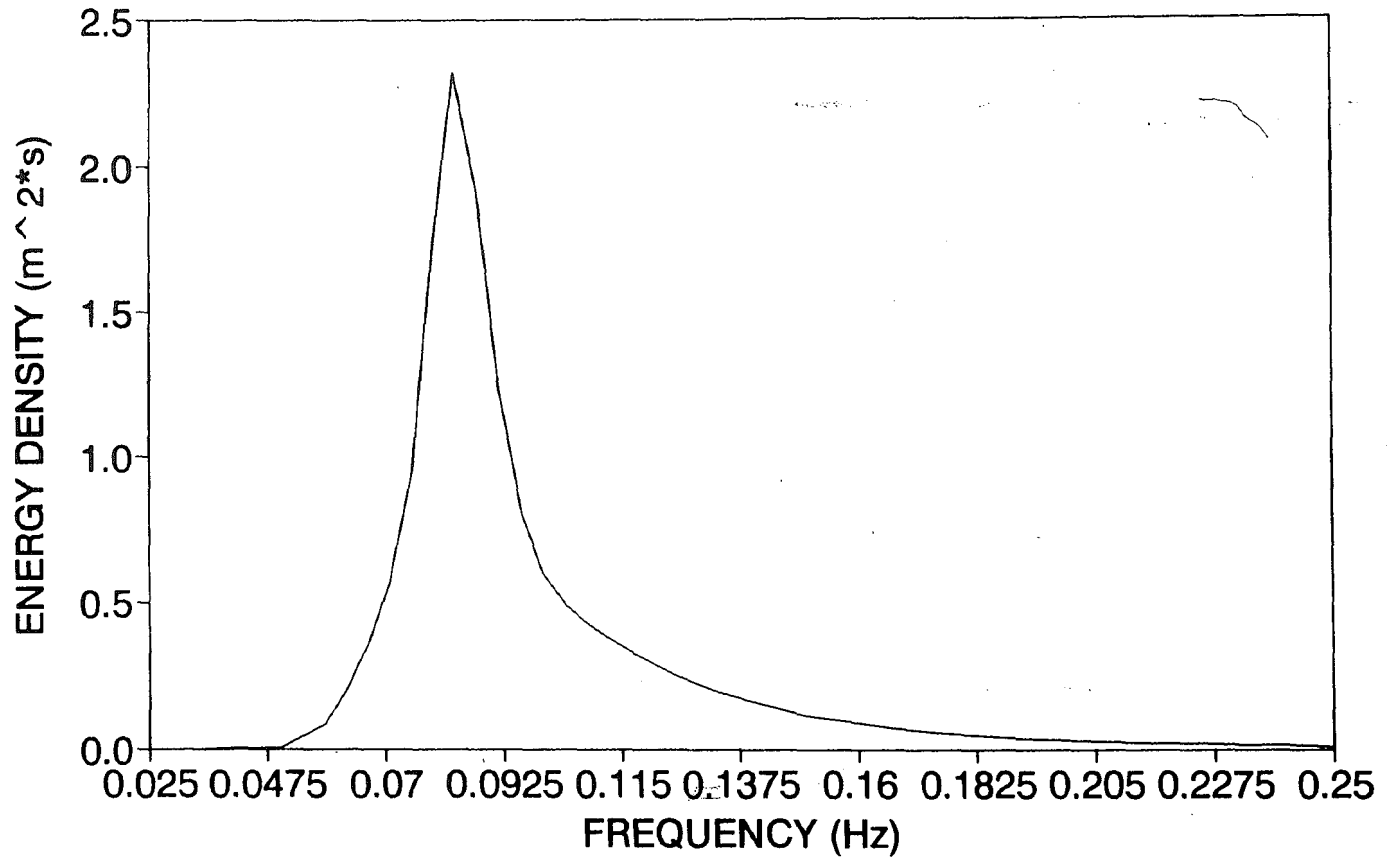


Figure 5.3 JONSWAP Frequency Spectrum: Deep Water Wave Period - 12 seconds

$$G(\theta) = \frac{2}{\pi} \cos^2 \theta \quad (5.4)$$

Figure 5.4 demonstrates how this function distributes the spectral energy density with deviance in direction. It should be noted that the energy density with respect to frequency only changes in magnitude, not in shape, as the deviation from the mean propagation direction is varied.

A more commonly used directional spreading function is the Mitsuyasu (1975) function. This function, given by Equation 5.5, is dependent not only upon the deviation from the mean propagation direction, but also upon deviation of frequency from the peak frequency.

$$G(f, \theta) = \frac{2^{2s-1} \Gamma^2(s+1)}{\pi \Gamma(2s+1)} \cos^{2s} \left(\frac{\theta}{2} \right) \quad (5.5)$$

where:

s directional spectrum spreading factor:

$$s = s_{\max} (f/f_p)^5 \quad \text{when } f < f_p$$

$$s = s_{\max} (f/f_p)^{-2.5} \quad \text{when } f > f_p$$

s_{\max} maximum value of s
 Γ mathematical gamma function

The maximum directional spectrum spreading factor increases as the wave steepness decreases. Thus, it would have its largest value at the edge of a storm and decrease continuously for swell propagating out from the storm. Goda (1985) recommends the

JONSWAP SPECTRUM COSINE SQUARED DISTRIBUTION

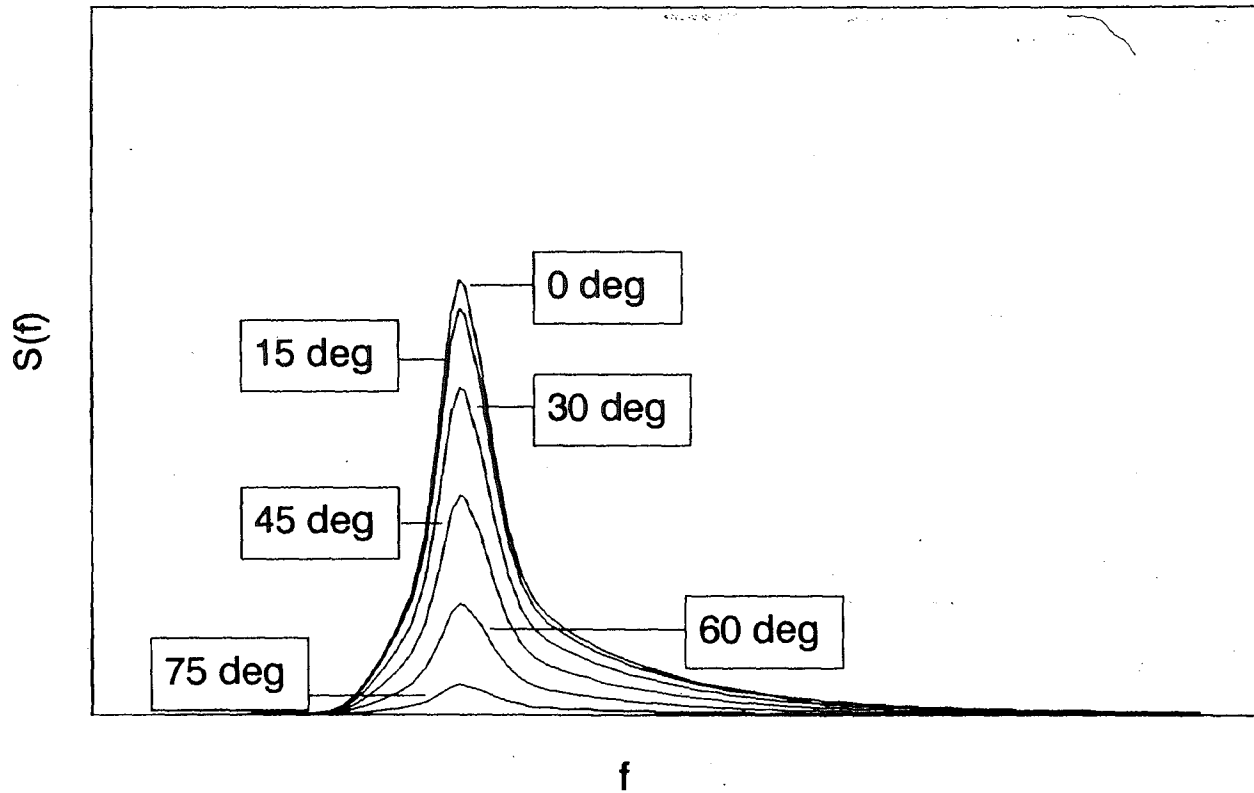


Figure 5.4 Cosine Squared Distribution (Sorensen (1993))

average value of 25 for the term s_{\max} for swell with a short decay distance. A representation of the Mitsuyasu (1975) spreading function is given in Figure 5.5.

As Figure 5.5 indicates, the spectral energy density is distributed more with direction as the frequency deviates further from the peak frequency. In contrast to the cosine squared distribution, in the Mitsuyasu (1975) distribution, the energy density distribution with respect to frequency is not constant as the deviation from the mean direction is varied.

5.3 Component Analysis

To obtain the effective combined refraction and shoaling coefficient for the nearshore directional spectra, the component analysis detailed in Chapter 2 is utilized. Both the directional spectra with a cosine squared distribution and the directional spectra with a Mitsuyasu (1975) distribution are used; however, there is some variation in the use of the component method for each directional distribution. The following sections discuss the procedure used on each directional distribution.

5.3.1 Cosine Squared Directional Distribution

The component analysis requires the use of frequency and direction bands to divide the directional spectrum into segments. This study uses 10 frequency bands and 17 direction bands. The direction bands have an equal spacing of 10° covering a directional spread from -85° to 85° about the mean propagation direction. Because

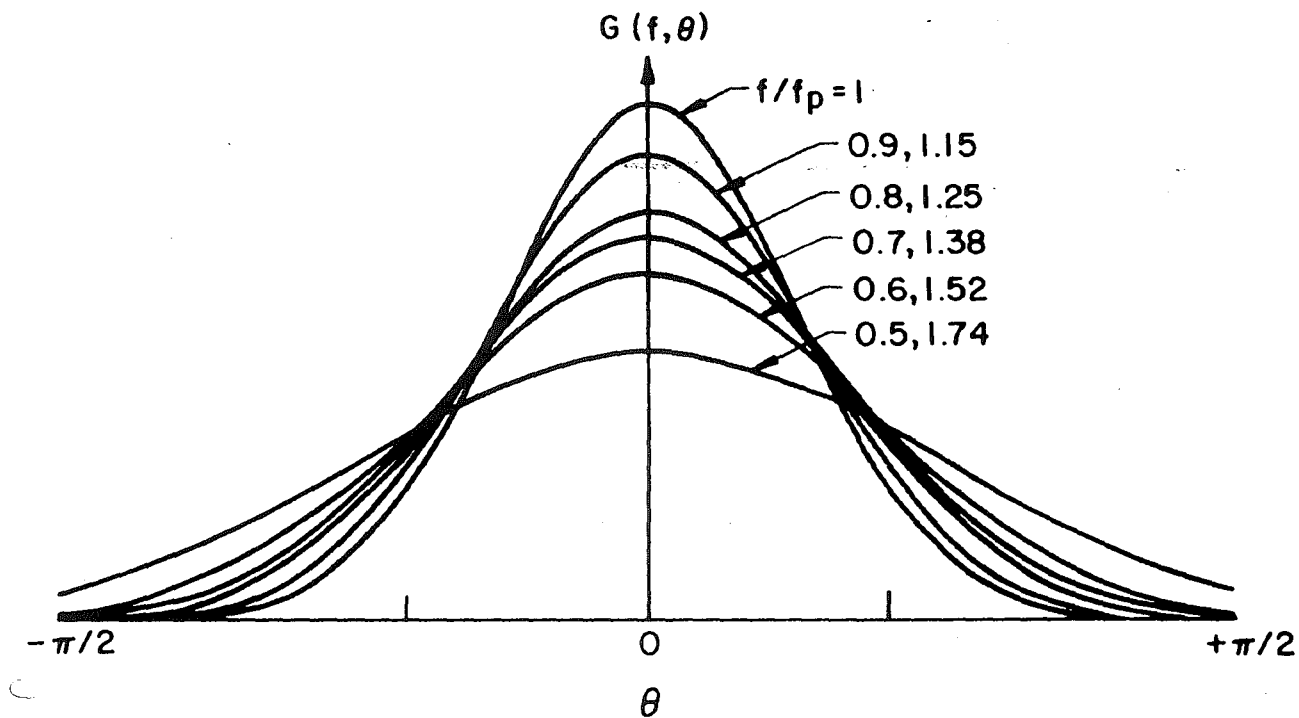


Figure 5.5 Mitsuyasu (1975) Distribution

the shape of the spectral energy density curve for a cosine squared directional distribution does not change with direction, it is easiest to divide the directional spectrum into components of equal energy with respect to frequency. This is illustrated in Figure 5.6 where the spacing of the frequency bands is a maximum near the edges of the spectrum and a minimum near the peak of the spectrum. By using this type of a division of the spectrum, the relative energy term, ΔE , will only change with deviance from the mean direction.

Once the spectrum has been divided into components, the relative energy of each wave component is calculated from Equation 2.7 by direct integration using a mathematical applications computer program, Mathcad 3.1. Then each component's representative frequency, f_{ij} , is calculated again with the use of a Mathcad 3.1 to solve Equation 5.6.

$$f_{ij} = \frac{\int_{\Delta f} \int_{\Delta \theta} f S(f, \theta) d\theta df}{\int_{\Delta f} \int_{\Delta \theta} S(f, \theta) d\theta df} \quad (5.6)$$

The component's representative direction, θ_{ij} , is taken at the center of the direction increment.

The representative frequency and direction for each component is then propagated into the nearshore using RCPWAVE. The resulting nearshore wave height for each component is then converted into a combined refraction and shoaling coefficient representative of the component, and Equation 2.6 is used to generate the

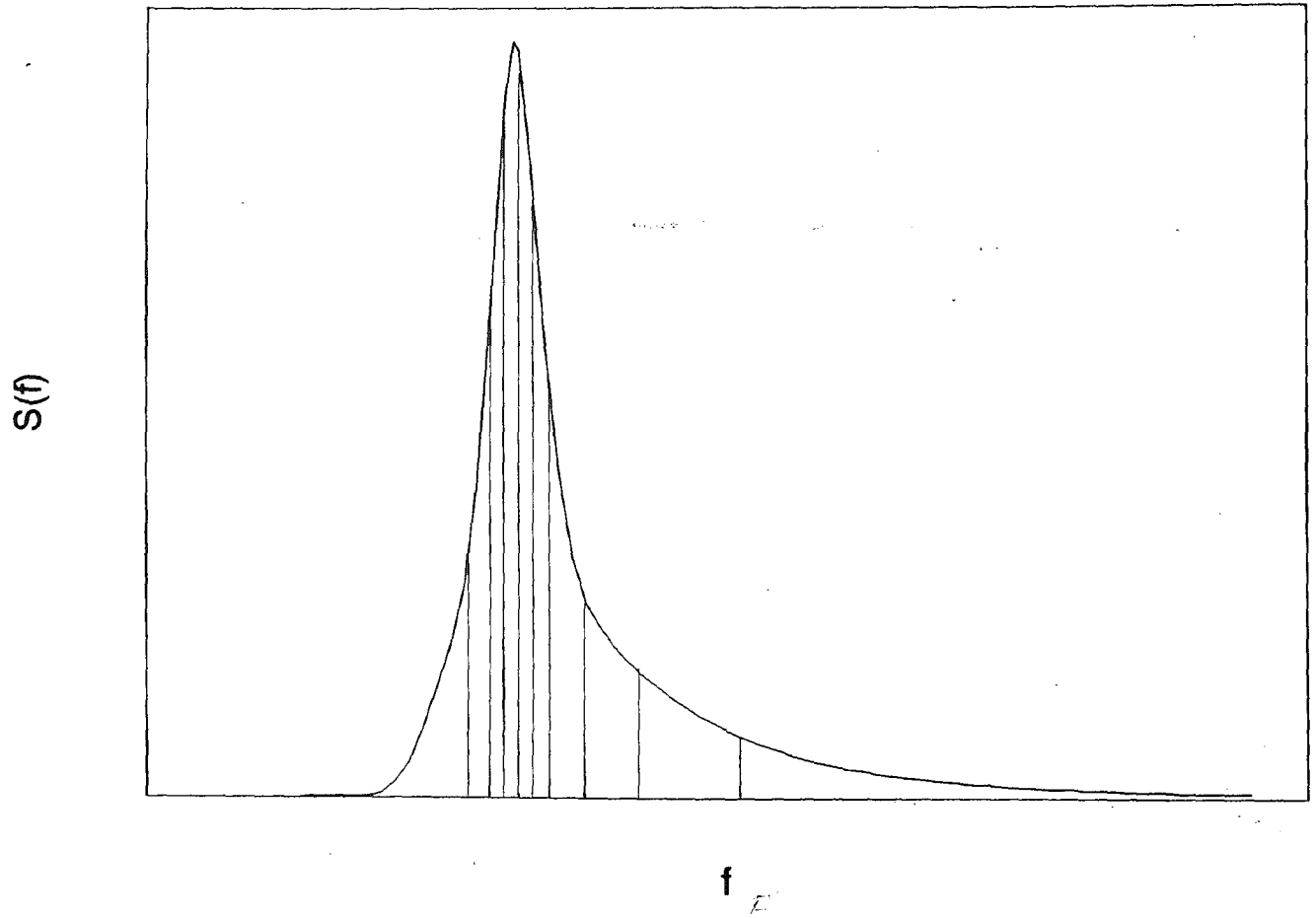


Figure 5.6 Frequency Band Division for the JONSWAP Spectrum with a Cosine Squared Distribution

effective combined refraction and shoaling coefficient for the nearshore location. The resulting nearshore propagation directions are then used as input into Equation 2.10 to determine the mean nearshore propagation direction. Each nearshore energy component is still represented by the same representative frequency as its respective deep water energy component. Using an equation similar Equation 2.10, the spectral peak frequency representative of the nearshore energy spectrum can be determined.

5.3.2 Mitsuyasu (1975) Directional Distribution

Similar to the analysis on the cosine squared function, the component analysis for a directional spectrum based on the Mitsuyasu (1975) function also uses 10 frequency bands and 17 direction bands and takes an equal direction band spacing of 10° . Unlike the cosine squared distribution, the frequency bands are equally spaced yielding a different relative energy term for each component of the directional spectrum.

Due to the complexity of the Mitsuyasu (1975) directional spreading function, it is necessary to graphically approximate the representative frequency for each wave component. Again, the representative direction is taken at the center of the direction increment. The relative energy for each wave component is approximated with Equation 5.7 which uses the representative spectral energy density of the wave component, $S(f_{ij}, \theta_{ij})$, as seen in Figure 2.5.

$$\Delta E_{ij} = \frac{\Delta f \Delta \theta S(f_{ij}, \theta_{ij})}{\sum_{i=1}^M \sum_{j=1}^N \Delta f \Delta \theta S(f_{ij}, \theta_{ij})} \quad (5.7)$$

The analysis then continues as with the cosine squared distribution resulting in an effective combined refraction and shoaling coefficient for the nearshore spectrum.

5.4 Results

The effective combined refraction and shoaling coefficients generated for the nearshore directional spectra are given in Table 4.

EFFECTIVE COMBINED REFRACTION AND SHOALING COEFFICIENT - $(K_r K_s)_{\text{eff}}$ Directional Spectral Propagation Analysis				
Deep Water Propagation Direction (deg)	Deep Water $T_p = 7$ seconds		Deep Water $T_p = 12$ seconds	
	Cosine Squared	Mitsuyasu	Cosine Squared	Mitsuyasu
0	0.91	0.94	0.94	.98
15	0.92	0.93	0.96	.97
30	0.87	0.91	0.89	.92
45	0.82	0.88	0.82	.85
60	0.74	0.80	0.73	.75

Table 4

Table 5 gives the generated nearshore mean wave propagation direction calculated from Equation 2.10.

NEARSHORE MEAN SPECTRAL PROPAGATION DIRECTION (deg) Directional Spectral Propagation Analysis				
Deep Water Propagation Direction (deg)	Deep Water $T_p = 7$ seconds		Deep Water $T_p = 12$ seconds	
	Cosine Squared	Mitsuyasu	Cosine Squared	Mitsuyasu
0	0	0	0	0
15	7	7	2	3
30	12	11	6	7
45	20	19	11	12
60	26	25	16	17

Table 5

Unlike with a monochromatic wave propagation, there are shifts in the peak wave frequency as a directional spectrum is moved into the nearshore. These nearshore peak wave frequencies, based on the nearshore directional spectral distribution, are given in Table 6 along with their respective peak wave periods.

NEARSHORE SPECTRAL PEAK FREQUENCY AND PERIOD Directional Spectral Propagation Analysis								
Deep Water Propagation Direction (deg)	Deep Water $T_p = 7$ seconds				Deep Water $T_p = 12$ seconds			
	Cosine Squared		Mitsuyasu		Cosine Squared		Mitsuyasu	
	f (Hz)	T_p (sec)	f (Hz)	T_p (sec)	f (Hz)	T_p (sec)	f (Hz)	T_p (sec)
0	0.23	4.3	0.25	4.0	.12	8.0	.14	7.4
15	0.23	4.3	0.25	4.0	.12	8.1	.13	7.4
30	0.23	4.3	0.25	4.1	.12	8.1	.13	7.5
45	0.23	4.3	0.25	4.0	.12	8.1	.13	7.5
60	0.23	4.3	0.25	4.0	.12	8.1	.13	7.5

Table 6

6.0 COMPARISON OF RESULTS

The following sections will discuss and compare the nearshore wave conditions generated from both a monochromatic wave propagation analysis and a directional spectral wave propagation analysis. Specifically, these sections will include the combined refraction and shoaling coefficients, peak period, and mean propagation direction.

6.1 Nearshore Combined Refraction and Shoaling Coefficient

Figures 6.1 and 6.2 graphically illustrate the generated results for the nearshore combined refraction and shoaling coefficients versus their respective deep water mean propagation direction. Figure 6.1 is for the test wave conditions with a 7 second deep water wave period, while Figure 6.2 is for those test conditions with a 12 second deep water period.

For the monochromatic systems as well as both directional spectral systems, the combined refraction coefficient follows a decreasing trend with respect to an increase in the deep water mean propagation direction. The deviation between the two approaches is most probably a result of the spectral energy lost from energy propagation offshore. Each spectral energy component with a propagation direction directed offshore is lost when the spectrum is moved into the nearshore. For the test conditions having a 7 second deep water period, this difference in the combined refraction and shoaling coefficients generated from a directional spectral wave propagation and those generated from a monochromatic wave propagation varies from

KrKs VS. MEAN DIRECTION

PEAK PERIOD = 7 seconds

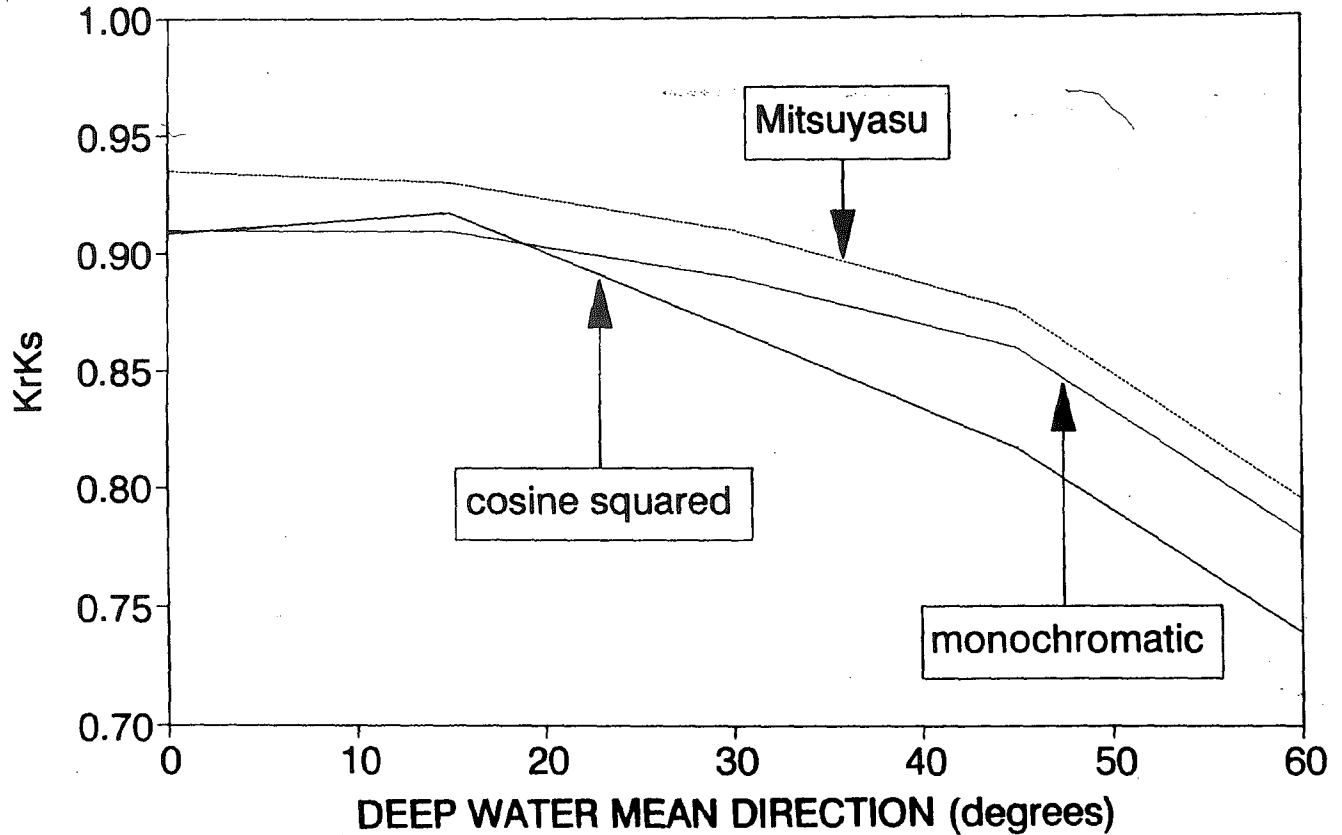


Figure 6.1 Combined Refraction and Shoaling Coefficient Versus Deep Water Mean Propagation Direction: Deep Water Wave Period - 7 seconds

KrKs VS. MEAN DIRECTION

PEAK PERIOD = 12 seconds

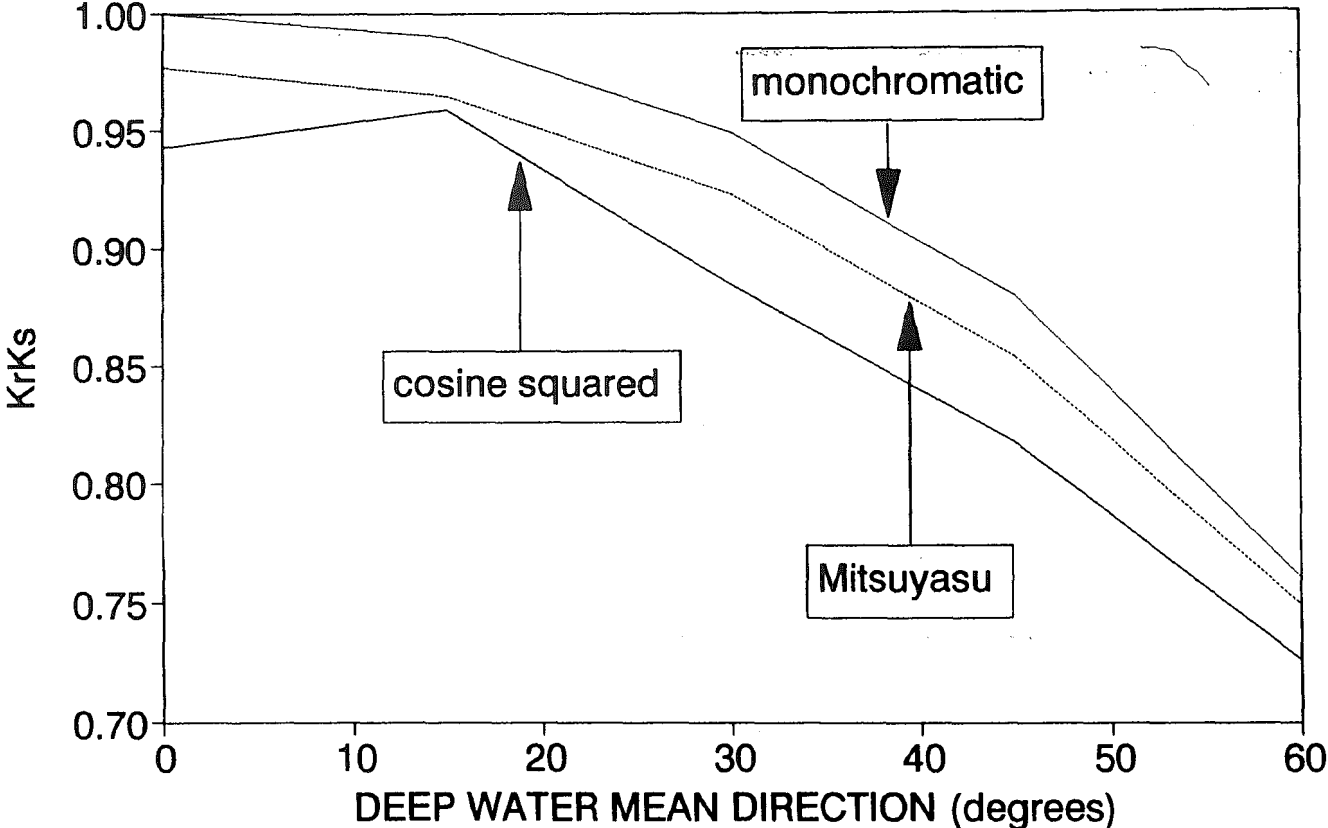


Figure 6.2 Combined Refraction and Shoaling Coefficient Versus Deep Water Mean Propagation Direction: Deep Water Wave Period - 12 seconds

0.01 to 0.04; whereas, for the 12 second deep water period, this difference varies from 0.01 to 0.06. The larger deep water period, 12 seconds, gives larger values of the combined refraction and shoaling coefficient for smaller deep water mean propagation directions, but as the deep water mean propagation direction is increased, the coefficient for the larger period wave system approaches that generated for the smaller period system, 7 seconds.

As these figures indicate, the directional spectral combined refraction and shoaling coefficient is dependent upon the which directional spreading function is employed. With respect to the monochromatic wave propagation analysis, the directional spectral analysis using a cosine squared function generally yields lower values for the combined refraction and shoaling coefficient for both deep water wave periods.

With the cosine squared distribution, it should be noted that the decreasing trend of the refraction and shoaling coefficient is broken around a mean propagation direction of 15° . At this location, the combined refraction and shoaling term increases approaching those values generated from the monochromatic propagation analysis, and for the wave period of 7 seconds, this term becomes larger than its equivalent from the monochromatic system.

The Mitsuyasu directional spreading function yields a continual decrease in the combined refraction and shoaling coefficient as the deep water mean propagation direction increases. With respect to the monochromatic propagation analysis, the directional spectral propagation analysis employing this distribution gives consistently

higher values for the shorter period wave cases and consistently lower values for the larger period cases.

In comparing the results generated from the cosine squared distribution with those generated from the Mitsuyasu distribution, it is necessary to consider the treatment of each distribution for this analysis. The procedure that is followed for each distribution is given in Chapter 5. A more accurate method is employed for obtaining result for the cosine squared distribution; whereas, an approximation method is employed for the Mitsuyasu distribution. Because of this inconsistency, a comparison between the generated results of these two directional distributions may be inconclusive. However, it is clear that the type of directional distribution employed can significantly effect the combined refraction and shoaling coefficient.

6.2 Nearshore Peak Period

For the monochromatic wave propagation analysis, the peak wave period is taken as a constant as the wave is propagated into the nearshore; however, when a directional spectrum is propagated into the nearshore, shifts in spectral energy cause changes in the peak wave period. The generated nearshore peak wave periods versus the deep water mean propagation direction for the 10 test wave conditions are plotted in Figures 6.3 and 6.4. Figure 6.3 represents the test conditions with a 7 second deep water wave period, while Figure 6.4 represents the test conditions with a 12 second deep water wave period.

NEARSHORE PEAK PERIOD

DEEP WATER PERIOD = 7 seconds

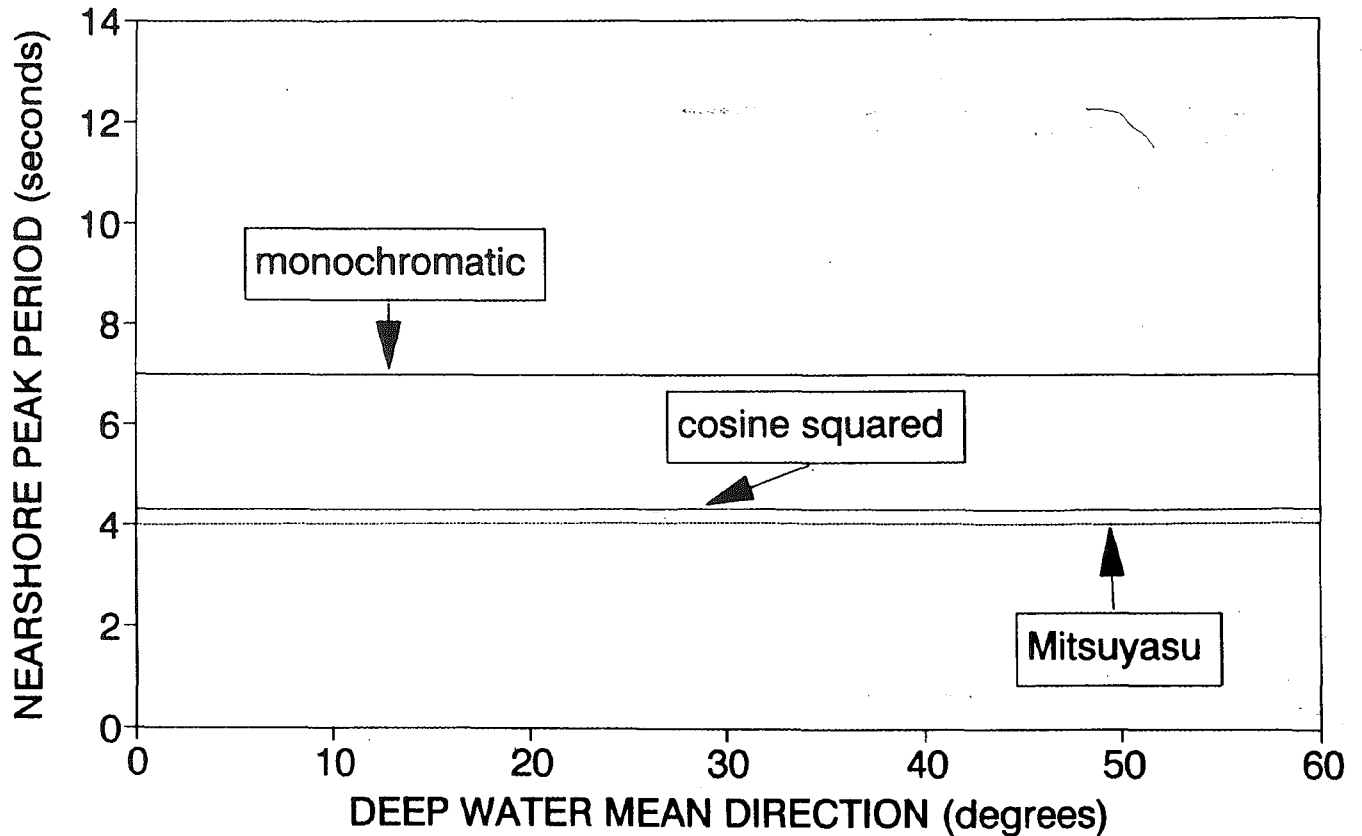
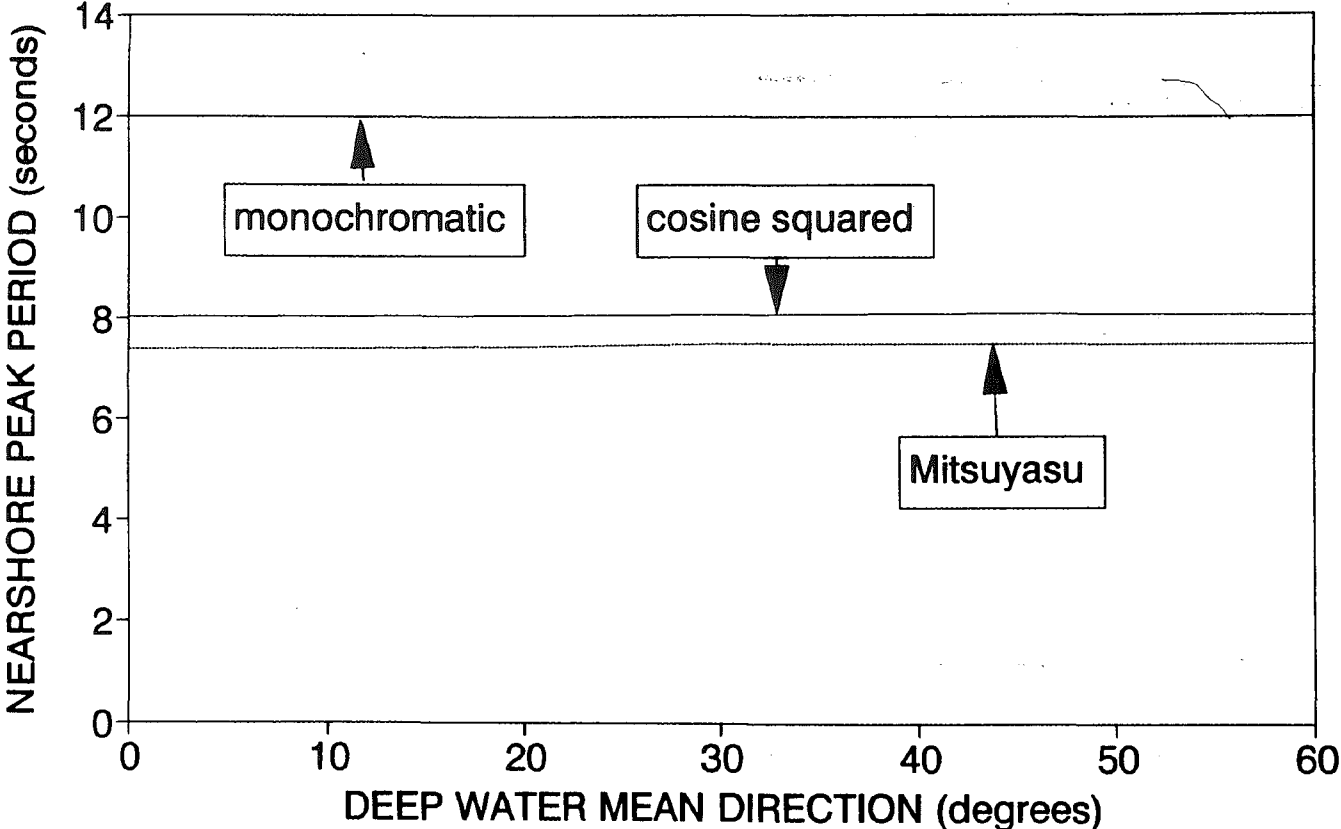


Figure 6.3 Nearshore Peak Wave Period Versus Deep Water Mean Propagation Direction: Deep Water Wave Period - 7 seconds

NEARSHORE PEAK PERIOD

DEEP WATER PERIOD = 12 seconds



58

Figure 6.4 Nearshore Peak Wave Period Versus Deep Water Mean Propagation Direction: Deep Water Wave Period - 12 seconds

As both figures indicate the nearshore peak wave period holds constant as the deep water propagation direction is varied for both the monochromatic propagation analysis and the directional spectral wave propagation analysis. However, for both deep water peak wave periods, the results generated by the directional spectral propagation yield a lower peak period than that given by a monochromatic propagation. This is indicative of a shift in spectral energy toward higher frequencies as the wave spectrum is moved into the nearshore. Again, this is in part a function of the spectral energy lost from propagation offshore.

When comparing the two directional distributions of the energy spectra against each other, it is clear that their effects on the nearshore peak wave period prediction are inconsequential. For both deep water peak periods, the cosine squared directional distribution yields a higher value than that generated from the Mitsuyasu directional distribution, but the magnitude of this difference may be considered negligible.

6.3 Nearshore Mean Propagation Direction

The nearshore mean propagation direction versus the deep water mean propagation direction for the 7 second and 12 second deep water wave period test conditions are presented in Figures 6.5 and 6.6, respectively. These figure indicate that as the wave propagates into the nearshore its propagation direction moves toward 0° . With respect to both directional spectral wave propagation analyses, the monochromatic wave propagation analysis consistently predicts larger nearshore mean propagation directions. The deviation of the results generated by the monochromatic

NEARSHORE MEAN DIRECTION

DEEP WATER PERIOD = 7 seconds

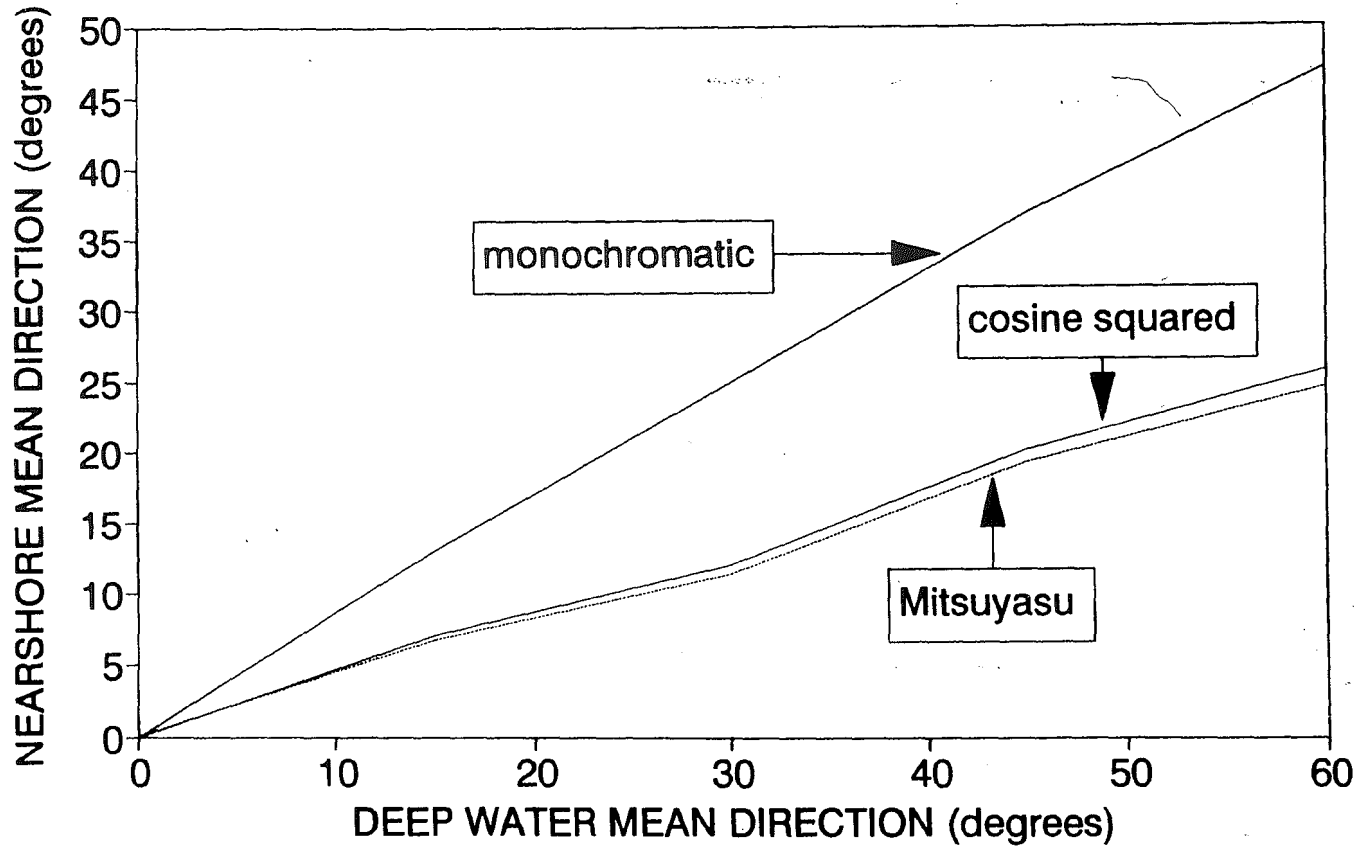


Figure 6.5 Nearshore Mean Propagation Direction Versus Deep Water Mean Propagation Direction: Deep Water Wave Period - 7 seconds

NEARSHORE MEAN DIRECTION

DEEP WATER PERIOD = 12 seconds

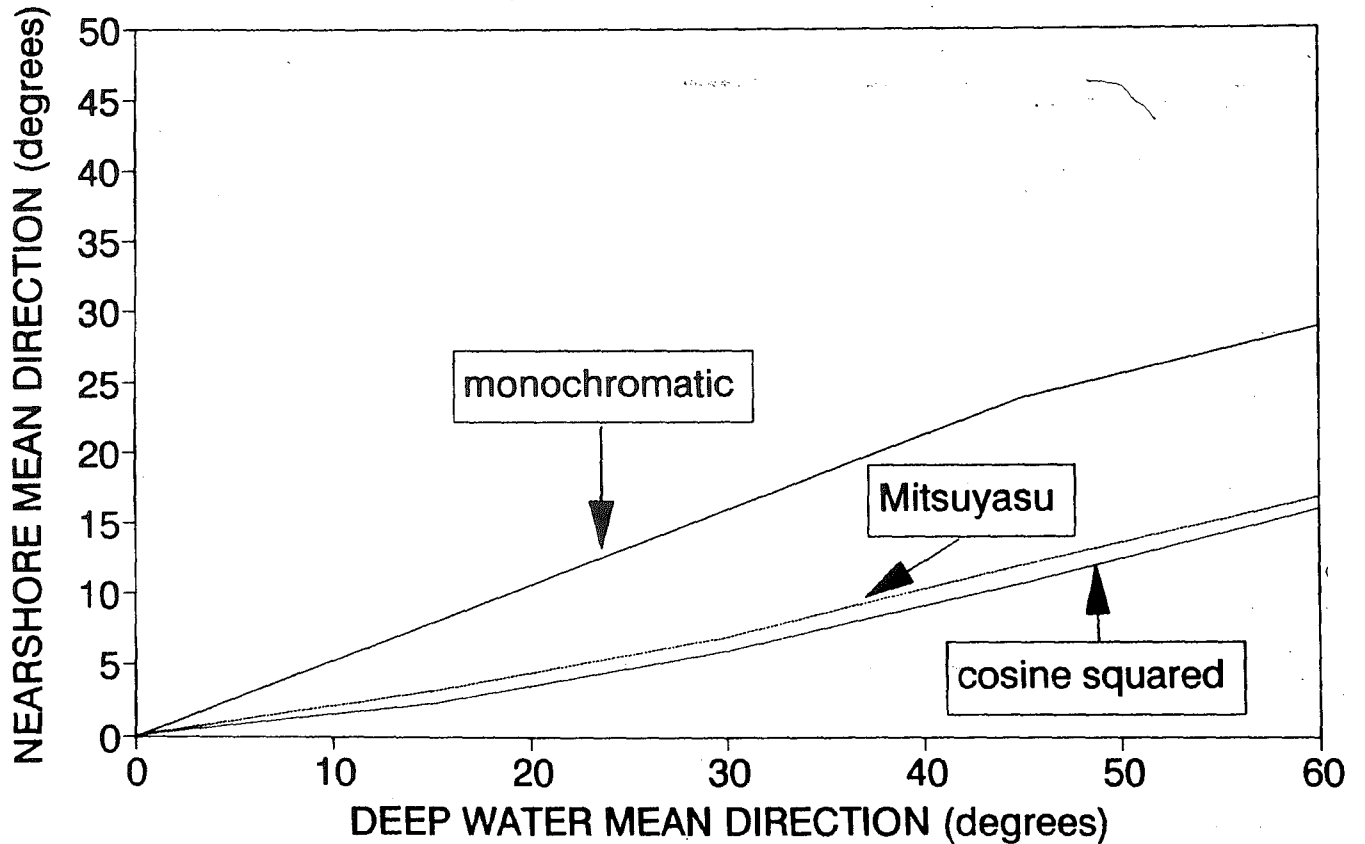


Figure 6.6 Nearshore Mean Propagation Direction Versus Deep Water Mean Propagation Direction: Deep Water Wave Period - 12 seconds

analysis from those generated by the directional spectral analysis increases as the deep water propagation direction increases, with the maximum deviation between the two analyses being over 20° . This deviation is much greater for the 7 second deep water wave period test conditions than for the 12 second conditions. These results indicate that a directional spectral wave propagation analysis yields more refractive effects than a monochromatic wave propagation analysis. Again, this deviation in the generated results is a consequence of the spectral energy shifts included with the directional spectral wave propagation analysis as well as a consequence of the spectral energy lost from energy propagation offshore.

As with the nearshore peak wave period, the directional spreading function applied to the energy spectrum has little effect on the final nearshore propagation direction. As Figures 6.5 and 6.6 indicate the differences between the propagation directions predicted using the cosine squared distribution and those predicted using the Mitsuyasu distribution vary less than 2° . For the test conditions with a 7 second deep water wave period, the cosine squared distribution yields slightly higher results than those generated by the Mitsuyasu distribution. The opposite is true for the test conditions based on a 12 second deep water wave period.

7.0 CONCLUSIONS

7.1 Impact on Coastal Design

The significant wave conditions used in coastal design need to be selected so as to best represent what is truly occurring in the field. These conditions should be chosen so that the proposed design is conservative while remaining economically efficient.

7.1.1 Wave Height

Wave height is important in coastal design because it generates the design loading to the coastal structure. The results obtained in this investigation show that a monochromatic wave propagation analysis will yield combined refraction and shoaling coefficients similar to those generated from a directional spectral wave propagation. These combined refraction and shoaling coefficients are directly related to the nearshore wave height via Equation 1.4. For most test conditions, the monochromatic wave propagation analysis gives slightly larger wave heights, yielding a conservative estimate for the design wave height. When considering the accuracy of the deep water wave conditions used as input into a propagation analysis, any differences between the nearshore wave height prediction given from a monochromatic analysis and that given from a directional spectral analysis are insignificant.

7.1.2 Wave Period

A directional spectral wave propagation analysis consistently generates nearshore peak wave periods lower than those generated by a monochromatic propagation analysis. The most significant impact of this with respect to engineering design lies in the fact that a lower period, or higher frequency, effects the wave steepness (H/L). Wave steepness is important when considering wave runup, beach response, and breaking regime. An increase in wave period can also cause the loading to a coastal structure to occur more frequently which can ultimately decrease the life of the structure. It is therefore important to consider the directional spectral distribution of the wave energy in coastal design.

7.1.3 Wave Propagation Direction

The wave propagation direction is important in the prediction of coastal sediment transport. As the wave propagation direction deviates further from 0° , the sediment transport load increases. Because a directional spectral wave propagation analysis, with respect to a monochromatic wave propagation analysis, significantly reduces the nearshore wave propagation direction, it is important to consider its effects in coastal design. A wave propagation direction generated by monochromatic analysis may lead to gross over prediction of sediment transport rates which could result in an economically inefficient coastal project. With respect to the nearshore wave propagation direction, it is important to consider the directional variation in propagation direction.

7.2 Recommendations for Further Analysis

It is apparent that there is some discrepancy between the two directional distributions used in the directional spectral wave propagation analysis; therefore, further analysis should be conducted to eliminate this discrepancy. It is suggested that the methods employed in this investigation be tested with directional spectral field data so as to better indicate the importance of using a directional spectral design condition.

Because the conclusions made from this investigation indicate the importance of variations in frequency and direction on coastal design, further investigation and development is needed to produce a time and cost efficient method for obtaining directional spectral wave conditions. Such an investigation could be based upon the concepts developed in the STWAVE finite difference based model.

REFERENCES

- Berkhoff, J. C. W. 1972. "Computation of Combined Refraction-Diffraction," Proceedings, 13th International Conference on Coastal Engineering, American Society of Civil Engineers, Vancouver, Canada.
- Bruun, P. 1954. "Coast Erosion and the Development of Beach Profiles," Technical Memorandum 44, Beach Erosion Board, U.S. Army Corps of Engineers, Washington, D.C.
- Cialone, M. A., Mark, D. J., Chou, L. W., Leenknecht, D. A., Davis, J. E., Lillycrop, L. S., Jensen, R. E. 1992. Coastal Modeling System (CMS) User's Manual, Instruction Report CERC-91-1, U.S. Army Corps of Engineers, Waterways Experiment Station, Vicksburg, MS.
- Davis, J. E., Smith, J. M., Vincent, C. L. 1991. Parametric Description for a Wave Energy Spectrum in the Surf Zone, Miscellaneous Paper CERC-91-11, U.S. Army Corps of Engineers, Waterways Experiment Station, Vicksburg, MS.
- Dean, R. G., Dalrymple R. A. 1984. Water Wave Mechanics for Engineers and Scientists, Prentice-Hall, Inc., Englewood Cliffs, NJ.
- Dean, R. G. 1987. "Coastal Sediment Processes: Toward Engineering Solutions," Proceedings, Coastal Sediments '87. American Society of Civil Engineers, New York, NY.
- Goda, Y. 1985. Random Seas and Design of Maritime Structures, University of Tokyo Press, Tokyo, Japan.
- Long, C. E. 1993. Storm Evolution of Directional Seas in Shallow Water - Draft Report, Miscellaneous Paper CERC-93, U.S. Army Corps of Engineers, Waterways Experiment Station, Vicksburg, MS.
- Mitsuyasu, H., Tasai, F., Subara, T., Mizuno, S., Ohkusu, M., Honda, T., and Rikiishi, K. 1975. "Observations of the Directional Spectrum of Ocean Waves Using a Clover-Leaf Bouy," Journal of Physical Oceanography, 5.
- Mitsuyasu, H., Tasai, F., Subara, T., Mizuno, S., Ohkusu, M., Honda, T., and Rikiishi, K. 1980. "Observations of the Directional Spectrum of Ocean Waves Using a Clover-Leaf Bouy," Journal of Physical Oceanography, 10.

Moore, B. D. 1982. Beach Profile Evolution in Response to Changes in Water Level and Wave Height. Department of Civil Engineering, University of Delaware, Newark, DE.

Sorensen, R. M. 1993. Basic Wave Mechanics: for Coastal and Ocean Engineers, John Wiley and Sons, Inc., New York, NY.

Tucker, M. J. 1991. Waves in Ocean Engineering: Measurement, Analysis, Interpretation, Redwood Press Ltd., Melksham, Wiltshire, Great Britain.

Work, P. A. 1991. "Effect of Varying Sediment Size on Equilibrium Beach Profiles," Proceedings, Coastal Sediments '91, Volume 1, American Society of Civil Engineers, New York, NY.

APPENDIX

VITA

JENNIFER L. IRISH

PLACE AND DATE OF BIRTH

Baltimore, Maryland
August 31, 1970

PARENTS NAMES

Thomas E. and Karen L. Irish

EDUCATION

M. S. in Civil Engineering 1994
Lehigh University Bethlehem, Pennsylvania
Primary Field of Study: Coastal and Hydraulic Engineering

B.S. in Civil Engineering, *with honors*, 1992
Lehigh University Bethlehem, Pennsylvania
Primary Field of Study: Civil Engineering
With Emphasis in Coastal and Hydraulic Engineering

PROFESSIONAL EXPERIENCE

June 1993 - U.S. ARMY CORPS OF ENGINEERS, WATERWAYS EXPERIMENT
August 1993 STATION, COASTAL ENGINEERING RESEARCH CENTER, FIELD
RESEARCH FACILITY, Duck, North Carolina
Contract Student. Assisted in field data collection, video imaging, and
computer analysis in areas of research including wave runup and Naval
mine defense; directed daily public tours.

June 1992 - U.S. ARMY CORPS OF ENGINEERS, WATERWAYS EXPERIMENT
August 1992 STATION, COASTAL ENGINEERING RESEARCH CENTER,
Vicksburg, Mississippi
Contract Student. Assisted in research, design, computer analysis, and
installation for coastal projects including overtopping analysis, harbor
channel sedimentation, and floating and detached breakwaters.

August 1992 -LEHIGH UNIVERSITY, CIVIL ENGINEERING DEPARTMENT,
May 1994 Bethlehem, Pennsylvania
Teaching Assistant. Conduct recitations and laboratory experiments,
review course work, and provide academic assistance for courses in
fluid mechanics and hydraulics.

HONORS AND AWARDS

Chi Epsilon Honorary Society, 1991.

1992 Recipient of the Elizabeth Major Nevius Award for "leadership,
citizenship, and scholarship."

Edward Twigg Memorial Scholarship, 1990/1991 and 1991/1992.

PROFESSIONAL SOCIETIES

American Water Resources Association - Lehigh University Student Chapter
Founding Member, President, Secretary.

American Society of Civil Engineers

Society of Women Engineers

END

OF

TITLE